
CarbonSense: A Multimodal Dataset and Baseline for Carbon Flux Modelling (Incomplete Manuscript)

Matthew Fortier
Mila Quebec
matthew.fortier@mila.quebec

Mats L. Richter
ServiceNow

Oliver Sonnentag
Université de Montréal

Chris Pal
Mila Quebec

Abstract

1 Understanding terrestrial carbon fluxes is essential for gaining insights into the
2 biosphere’s response to climate change and the capacity of ecosystems to absorb
3 anthropogenic CO₂ emissions. However, directly measuring these fluxes requires
4 long-term maintenance of field sensors, and the resulting data is typically for-
5 matted for ecological research, not for deep learning applications. To address
6 these challenges we present CarbonSense, the first machine learning-ready dataset
7 specifically designed for carbon flux modelling. Alongside this dataset, we present
8 a baseline model which achieves state-of-the-art performance in this domain. By
9 providing these resources, we aim to lower the barrier to entry for deep learning
10 researchers and stimulate advancements in data-driven carbon flux modelling.

11 1 Introduction

12 The biosphere plays a critical role in regulating Earth’s climate. Since the mid-20th century, terrestrial
13 ecosystems have absorbed up to a third of anthropogenic carbon emissions [1]. However, climate
14 change introduces uncertainty about the future resilience and capacity of these ecosystems. Under-
15 standing the carbon dynamics of our biosphere, and how those dynamics are changing in response
16 to climate change, will give crucial insight into the health of our ecosystems and their ability to
17 sequester carbon in the future.

18 Carbon fluxes describe the movement of carbon into and out of these ecosystems resulting from
19 processes like photosynthesis and cellular respiration. They are often analogised as the "breathing of
20 the biosphere" [2]. However, the large number of dependent processes makes these fluxes challenging
21 to simulate with process-based models¹. Normally, large scale observational data helps climate
22 scientists to parameterize their models, but carbon fluxes can only be measured in small areas with
23 long-term sensor deployment, creating a data bottleneck.

24 In recent years, machine learning techniques have been used to upscale carbon flux data using
25 meteorological and geospatial variables. This is known as data-driven carbon flux modelling (DCFM),
26 and it can be used to produce global carbon flux maps that are useful both as an end product for

¹Process-based models simulate biological, chemical, and physical processes using parameterized equations based on scientific understanding. Historically, the term "climate model" has referred to a process-based model as opposed to a machine learning model.

27 studying ecosystem health, and as a benchmark for improving process-based models [3]. Most studies
 28 perform DCFM with random forests [4]–[6], XGBoost [7], or ensembles of similar methods [8], [9].
 29 But these models cannot fully capitalize on the multimodality of the input data, often resorting to
 30 heavy compression techniques that compromise the quality of the end product.

31 Deep learning techniques could vastly improve our ability to model carbon fluxes. Multimodal
 32 models have been successfully applied to many niche domains [10] such as clinical diagnostics [11],
 33 land use cover classification [12], and wildfire surface fuel estimates [13]. Bridging the gap between
 34 the deep learning and carbon dynamics research communities will require a sustained effort, but the
 35 benefit to our understanding of the changing climate will be substantial.

36 Our work seeks to establish a foothold for deep learning research in DCFM and lower the barrier to
 37 entry for future researchers by providing the following:

- 38 • An overview of DCFM for deep learning researchers (Section 2)
- 39 • A multimodal ML-ready dataset for DCFM (Section 3)
- 40 • A baseline model which achieves state-of-the-art performance in DCFM (Section 4)

41 We will discuss our experiments in section 5 and provide guidelines for reporting results in this
 42 domain.

43 2 Data-Driven Carbon Flux Modelling

44 At its core, DCFM is a regression problem. The target (carbon flux) depends on many factors including
 45 ecosystem makeup, meteorological conditions, local topography and geology, and disturbances (fires,
 46 animal activity, etc). Meteorological data is easy to obtain, but the other predictors are challenging
 47 to measure and represent, especially at a global scale. Geospatial and semantic data are commonly
 48 employed as a proxy for the other predictors.

49 2.1 Measuring Fluxes

50 The most common technique for measuring
 51 fluxes is eddy covariance (EC) [14]. This is a mi-
 52 crometeorological technique where researchers
 53 erect a tower (typically above canopy height)
 54 and mount sensors which measure atmospheric
 55 gas fluxes across small turbulent vortices ("ed-
 56 dies"). A simplified EC station is depicted in
 57 Figure 1. CO₂ and water vapour are the most
 58 widely measured, but some towers also mea-
 59 sure methane (CH₄) [4], [5] or nitrous oxide
 60 (N₂O) [15]. Our work focuses on CO₂ due to
 61 the prevalence of standardized data collections.

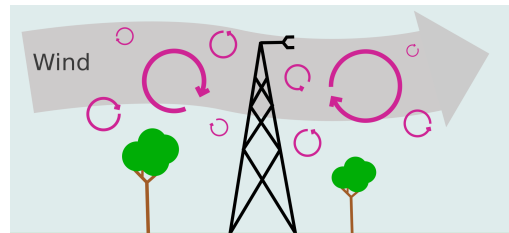


Figure 1: Simplified EC station. Sensors measure atmospheric CO₂ gradients across small sensors

62 Carbon fluxes can be recorded and expressed
 63 in many ways, but most represent the movement of carbon in terms of mass / area / time (ex
 64 $g \cdot C \cdot m^{-2} \cdot hr$). Gross primary productivity (GPP) refers to the total carbon uptake by plants for
 65 photosynthesis. Ecosystem respiration (RECO) is the total carbon returned to the atmosphere through
 66 both plant and microbial respiration. Net ecosystem exchange (NEE) is the net carbon flux from GPP
 67 and RECO; a carbon sink will have a negative NEE as more carbon is being consumed through GPP
 68 than released through RECO. NEE is the flux that is directly measured by EC stations, and for that
 69 reason will be the main focus of our experiments, but we provide GPP and RECO data in our dataset.

70 2.2 Flux Predictors

71 **Meteorological Data** DCFM meteorological data comes from EC stations. In addition to carbon
 72 fluxes, EC stations measure local atmospheric conditions such as wind velocity and direction,

73 precipitation, surface temperature, soil moisture, and others. The exact number and type of variables
74 depends on the site, but regional networks maintain a minimum mandatory set for researchers wishing
75 to submit their data [16]. For trained models looking to run global inference, meteorological variables
76 can be obtained from publicly available reanalysis products such as ERA5 [17] which provides the
77 variables on a 0.05 degree grid.

78 **Geospatial Data** Satellite imagery of the area surrounding an EC station can give useful information
79 about the land cover and ecosystem makeup. The most common products for DCFM are based on
80 Moderate Resolution Imaging Spectroradiometer (MODIS) data [18]. This satellite constellation
81 produces new imagery for Earth’s surface every 1-2 days and has 36 spectral bands with resolutions
82 varying between 250m and 1km. The MCD43A4 derived product is particularly common - it fuses
83 MODIS data in a 16-day sliding window to produce a single image each day. This not only helps
84 to address cloud coverage, but produces nadir BRDF-adjusted reflectance (NBAR) images which
85 remove angle effects from directional reflectance [19]. Each image therefore appears as it would
86 from directly overhead at solar noon. MCD43A2 is also widely used, which contains categorical
87 values for each pixel indicating snow and water cover [20]. The terms "geospatial data", "satellite
88 data" and "remote sensing data" are often used interchangeably.

89 **Semantic Data** Some models ingest semantic data such as ecosystem classification ("Croplands",
90 "Evergreen needleleaf forest", "Snow and ice", etc). These classifications follow standardized
91 schemes such as the International Geosphere-Biosphere Programme (IGBP). Ecosystem classification
92 is performed by domain experts, but some MODIS products coarsely approximate this information
93 on a global grid [21], allowing this data to also be used for global inference.

94 **3 The CarbonSense Dataset**

95 We provide the first ML-ready dataset for DCFM, CarbonSense. CarbonSense consists of EC station
96 data and corresponding MODIS geospatial data for 385 sites across the globe, totalling over 27
97 million hourly observations. This section covers our data sources, processing pipeline, and usage
98 guidelines.

99 **3.1 Data Collection**

100 All meteorological data was aggregated from major EC data networks, including FLUXNET 2015
101 [16], the Integrated Carbon Observation System (ICOS) 2023 release [22], ICOS Warm Winter
102 release [23], and Ameriflux 2023 release [24]. These source datasets were chosen due to their use of
103 the ONEFlux processing pipeline [16], ensuring standardized coding and units. A map of EC sites
104 and their source networks is shown in Figure 2. North America and Europe are over-represented in
105 this site list due greater data accessibility, and we discuss the implications of this in section 3.3.

106 Geospatial data in CarbonSense are sourced from MODIS products. Specifically, we utilize the seven
107 spectral bands from the MCD43A4 product [19], as well as the water and snow cover bands from
108 MCD43A2 [20]. Following the guidelines from [18], we extract images in a 4km by 4km square
109 centered on each EC station. Given a spatial resolution of 500m per pixel, this yields an 8x8 pixel
110 image with 9 channels for every site-day.

111 **3.2 Data Pipeline**

112 The first stage in the pipeline is EC data fusion. Many sites had overlapping data from different
113 source networks. For example, the site Degero in Sweden (SE-Deg) had data from 2001-2020 in the
114 ICOS Warm Winter release, and data from 2019-2022 in the ICOS 2023 release. Data were fused
115 with overlapping values taken from the more recent release as in previous DCFM work [7]. Any
116 sites which report half-hourly data were downsampled to hourly at this stage, and daily and monthly
117 recordings were discarded.

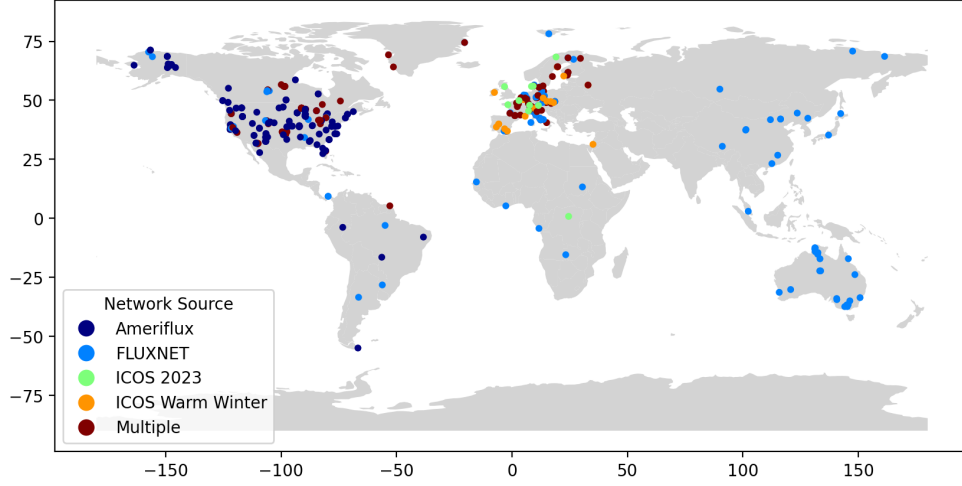


Figure 2: Global map of eddy covariance sites used in CarbonSense, with corresponding source networks. Some sites were present in multiple networks.

118 Once fused, we extracted the relevant time blocks for each EC station along with its geographic
 119 location. This metadata was used to obtain the appropriate MODIS data for each site. Data was
 120 pulled procedurally from Google Earth Engine [25].

121 Meteorological data was pruned to remove unwanted variables. Some, like soil moisture and
 122 temperature, were either unavailable for most sites or were heavily gap-filled. We removed these
 123 variables in order to reduce the risk of compounding errors on the underlying pipeline gapfilling
 124 techniques. A full list of variables at this stage is given in table 6.

125 As a final stage in the pipeline, we apply a min-max normalization on predictor variables. We map
 126 cyclic variables (those with a cyclic range such as wind direction) to the range $[-1, 1)$ and acyclic
 127 variables to the range $[-0.5, 0.5)$. This normalization procedure is conducive to our Fourier encoding
 128 method discussed in section 4.1.

129 We offer CarbonSense both before ("raw") and after ("normalized") our normalization step. Our
 130 pipeline can be configured to have variable "leniency" for gap-filled values. Those who wish to use
 131 CarbonSense with strictly observed values may do so at the cost of a smaller number of samples. The
 132 full pipeline code is also available so that researchers can add more source networks with minimal
 133 modifications. A diagram of the entire pipeline is shown in Figure 3, and we provide a more detailed
 134 description of all these steps in the supplementary material.

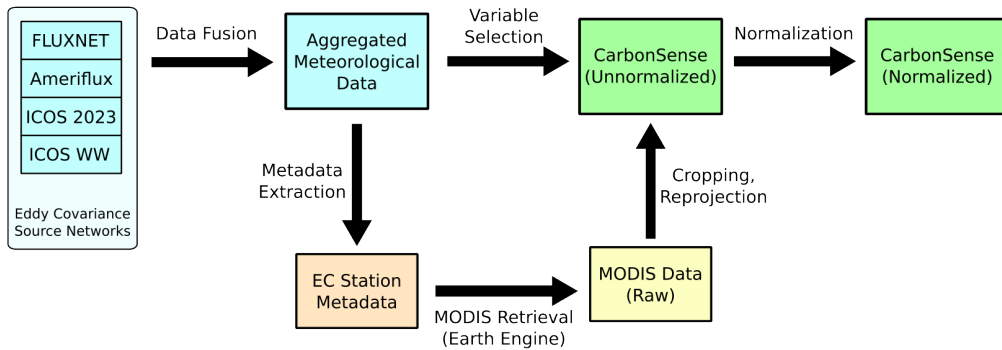


Figure 3: Data pipeline used to create CarbonSense from EC and MODIS data.

3.3 Using the Dataset

Site Sampling The geographic and ecological distribution of sites remains a challenge in statistical CFM, and CarbonSense is no different. Given the significant overrepresentation of certain regions (North America, Europe) and ecosystems (evergreen needleleaf forests, grasslands), we maintain a partitioned structure where each site has its own directory containing EC data, geospatial data, and metadata. Researchers may choose to select sites for training and validation which allow for fair out-of-distribution performance estimates, or to achieve a balanced sampling of ecosystems.

Dataloader We supply an example PyTorch dataloader for CarbonSense specifically tailored to our baseline model. Using the dataloader requires specifying which carbon flux to use as the target, which sites to include in each dataloader instance, and the context window length for multi-timestep training.

Licensing CarbonSense is available under the CC-BY-4.0 license, meaning it can be shared, transformed, and used for any purpose given proper attribution. This is an extension of the same license for all three source networks, and MODIS data is provided under public domain. We feel that permissive licensing is essential in order to foster greater scientific interest in CFM in the deep learning community.

4 The EcoPerceiver Architecture

In this section we present EcoPerceiver, a multimodal architecture for CFM. The state-of-the-art for CFM are simple tabular methods, and we felt it would be appropriate to include a baseline model which demonstrates how deep learning concepts can be leveraged for this unique problem domain.

EcoPerceiver is based on the Perceiver architecture [26], which cross attends a variable number of inputs onto a compact latent space, allowing for extreme input flexibility. Missing inputs are common in DCFM due to coverage gaps, outlier values, or failing sensors. Rather than rely on gapfilling techniques, we chose this architecture for its robustness to missing inputs.

We also wanted a model which could ingest data from a varying time window. All available DCFM models treat carbon dynamics as a Markovian process, predicting a flux value from immediate conditions. But biological processes are not Markovian; a plant’s rate of photosynthesis may depend on conditions hours or days into the past (or further!). Our model achieves this through the use of windowed cross attention, detailed below.

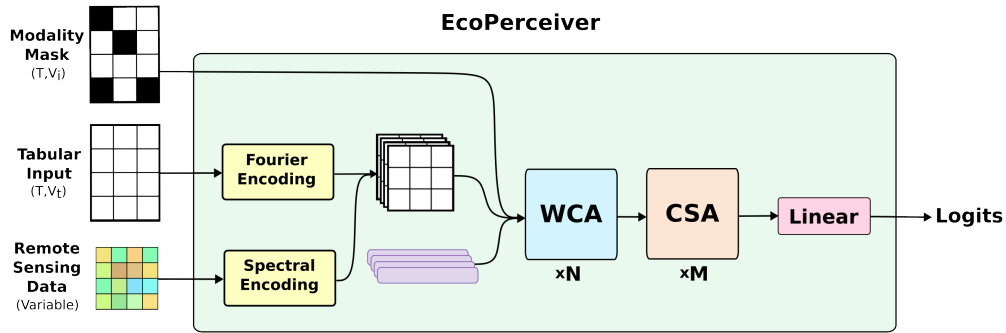


Figure 4: Overview of EcoPerceiver architecture.

4.1 Data Ingestion

Small fluctuations in meteorological variables have the potential to influence ecological processes. For this reason, it is important that the model is sensitive to small changes in input values. We take

167 inspiration from NeRF’s Fourier encoding [27] which maps continuous values to higher dimensional
 168 space with high frequency sinusoids. As discussed previously, cyclic variables in CarbonSense are
 169 mapped to $[-0.5, 0.5]$ and acyclic variables are mapped to $[-1.0, 1.0]$. We start by taking each
 170 variable x , and applying it to a series of sinusoids to produce an encoded vector with:

$$f(x) = \left[\dots, \sin(2^k \pi x), \cos(2^k \pi x), \dots \right] \Big| k \in [0, K) \quad (1)$$

171 where K is a hyperparameter indicating the maximum sampling frequency. Higher values of K allow
 172 the model to better discern between small differences in input. With our normalization scheme, cyclic
 173 variables at values of -1 and 1 will produce identical vectors under this transform as intended.

174 Each input is given a learned embedding specific to the underlying variable. This is then concatenated
 175 with the Fourier encoding to produce a final input vector of length $H_i = 2K + l_{emb}$ for each input. It
 176 should be noted that EcoPerceiver requires a list of all possible observation types at creation time so
 177 that these embeddings can be created.

178 Geospatial data is similarly processed, except that each spectral band is flattened into a vector
 179 of length $2K$ via linear transformation instead of Fourier encoding. Each band is then given an
 180 embedding to produce a vector of length H_i .

181 The tabular and geospatial data are then stacked to create a matrix of shape (V_t, H_i) where V_t is the
 182 sum of the number of meteorological variables and spectral bands at timestep t . Since EcoPerceiver
 183 conditions on observations in a fixed context window of length T , the final data cube used for input to
 184 the attention layers is of shape (T, V_t, H_i) . Figure 5 gives a visualization of the encoding procedure.

185 Not every timestep has a value for every variable, and this is certainly true of geospatial data which
 186 is typically provided once per 24 hours. To account for this, EcoPerceiver takes a modality mask
 187 indicating which values to ignore in the cross attentive layers.

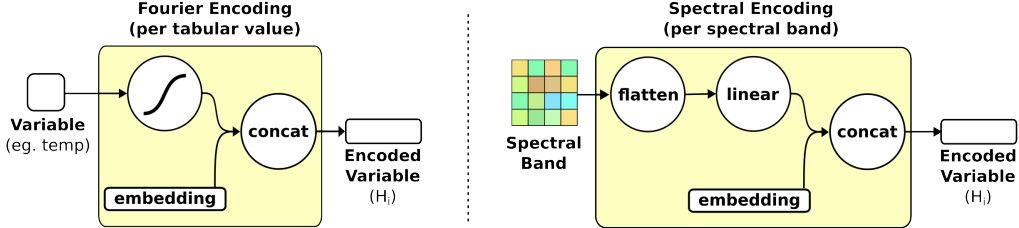


Figure 5: Input encoding for EcoPerceiver. Left: Tabular values are fed into the Fourier encoding function (1) and concatenated with an embedding. Right: Spectral bands are similarly processed except with linear projection instead of Fourier encoding.

188 4.2 Windowed Cross Attention

189 We build on Perceiver’s core concept of cross-attending data onto a compact latent space for process-
 190 ing. EcoPerceiver uses a latent space of size (T, H_l) where T is the context window length and H_l is
 191 the hidden token length (hyperparameter). Each token extracts input data via cross-attention from
 192 its respective timestep’s observations. In this way each token can be thought of as representing the
 193 ecosystem’s “state” in time, as it pertains to the carbon cycle.

194 This operation would be very inefficient with vanilla cross attention, as each token would use at most
 195 $\frac{1}{T}$ observations with an attention mask removing the rest. We take inspiration from SWin Transformer
 196 [28] and instead push the context window dimension (T) into the batch dimension for both input and
 197 latent space. The resulting Windowed Cross Attention (WCA) has a runtime of $O(T \cdot V_t \cdot H_a)$ where
 198 H_a is the projection dimension.

199 In keeping with Perceiver, each WCA operation is followed by a self-attention operation in the latent
 200 space. We pass a causal mask to the self attention so each timestep is conditioned only on past and

201 present observations. We refer to this as Causal Self Attention (CSA). This constitutes a full WCA
 202 block as shown in Figure 6.

203 WCA blocks are repeated N times, repeatedly cross attending inputs onto the latent space with self
 204 attention in between. We then apply a series of M CSA operations and use the final timestep’s token
 205 as input to a linear layer. The output of this is the estimate of the desired carbon flux.

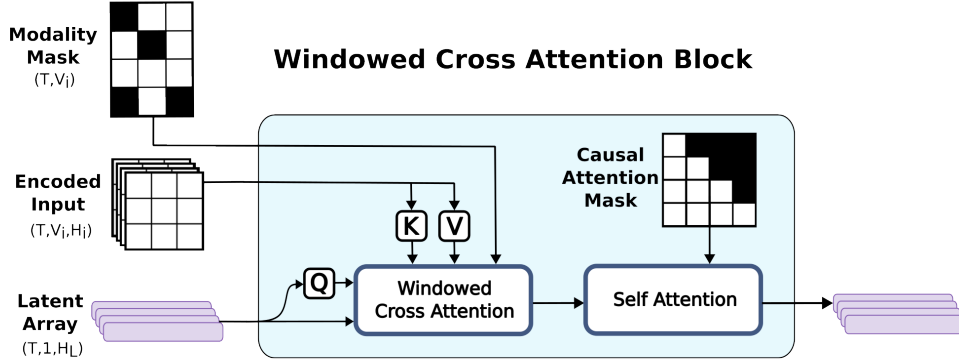


Figure 6: Windowed Cross Attention (WCA) block. Encoded inputs are cross-attended onto the latent space with a modality mask to indicate missing values. The time dimension is pushed into the batch dimension, so this operation is performed $B \cdot T$ times per batch. Causal self attention proceeds as normal.

206 4.3 Observational Dropout

207 Overconditioning on a small subset of variables could reduce EcoPerceiver’s ability to generalize.
 208 Since our architecture is robust to missing observations, we implemented an observational dropout
 209 scheme to combat this. Given a hyperparameter ($0 < \epsilon < 1$), we use the modality mask to randomly
 210 remove a portion of observations during training equal to ϵ (in addition to any missing observations).
 211 We find that this improves validation performance as seen in the ablation studies in Appendix B.

212 5 Experiments

213 In this section, we present a series of experiments using CarbonSense. Our analysis includes two
 214 models: an EcoPerceiver model as introduced in 4, and an XGBoost model implemented to mimic
 215 current state-of-the-art approaches in DCFM. We aim to demonstrate the power of tailored deep
 216 architectures for DCFM and establish a robust baseline that will support and inspire future research
 217 efforts. We also present guidelines for running similar experiments and presenting results.

218 5.1 Data Splitting

219 EC stations were randomly divided into train, validation, and test sets based on their IGBP classifica-
 220 tion. We wanted to keep at least 5 of each ecosystem type held out for testing, but several types did
 221 not have enough data to accommodate this. In particular, snow and ice (SNO), water bodies (WAT),
 222 cropland/vegetation mosaics (CVM) and deciduous needleleaf forests (DNF) only had 1 or 2 sites
 223 each, so we use them to measure the zero- and one-shot performance of our model.

224 The main focus of this research is on models trained *across* different ecosystem types, as opposed to
 225 other research studying CFM *within a single* type (ex: [4] [8] [9]). However, the partitioned nature of
 226 CarbonSenseaffords any researcher the ability to develop, for example, a model meant for grassland
 227 flux modelling. We give an example of this, along with other experimental results, in Appendix B.

5.2 Model Configurations

All experiments were performed on the Compute Canada cluster. To ensure accurate confidence intervals, we ran 10 experiments per model once optimal hyperparameters were found (as suggested by [29]).

EcoPerceiver experiments were each run on 4 A100 GPUs using dataset parallelization. We used the AdamW optimizer [30] with a learning rate of $8e-5$ and a batch size of 4096. A single warm-up epoch was performed followed by a cosine annealing learning rate schedule over 20 epochs. Most experiments converged between 4 and 10 epochs. Hyperparameters were initially selected by hand and then refined by experimental perturbation; methods such as random search were infeasible due to the large hyperparameter space, compute constraints, and lack of similar experiments to draw inspiration from.

XGBoost experiments were run on CPU nodes. Hyperparameters were found by random search over 50 iterations. Since XGBoost is a tabular algorithm, we prepared geospatial data in a similar fashion to XBASE [7]; each spectral band represents a single input value to the model. The value is obtained by taking a weighted average of pixels based on Euclidean distance from the center of the image. The code for this processing, as well as the final list of hyperparameters, is provided in the supplementary material.

Table 1: Number of EC sites in train / validation / test splits, by IGBP ecosystem type

IGBP	Train	Valid	Test
WET	34	8	5
DNF	0	0	1
WSA	7	1	2
EBF	8	1	4
ENF	64	15	6
DBF	34	8	5
CRO	36	8	5
MF	7	1	5
GRA	48	11	5
OSH	20	5	5
CVM	1	0	1
CSH	4	1	2
SAV	8	2	4
SNO	0	0	1
WAT	1	0	1

5.3 Reproducibility and Reliability

Both EcoPerceiver and XGBoost were trained with reproducibility in mind. Once optimal hyperparameters were found, we performed 10 experiments with each model in order to obtain a reliable measure of performance (inspired by [29]). Set seeds were provided to all frameworks utilizing RNG, and distributed dataloader workers were also seed-controlled to ensure full reproducibility of our results.

5.4 Metrics

The most commonly used performance metric in DCFM (and any form of hydrologic modelling) is the Nash-Sutcliffe Modelling Efficiency (NSE) [31], described with the following equation:

$$\text{NSE}(x) = 1 - \frac{\sum_i (y_i - x_i)^2}{\sum_i (y_i - \bar{y})^2} \quad (2)$$

where a value of 1 represents perfect correlation between x and y . A value of 0 represents the same performance as guessing the mean of y , and negative values indicate that the mean of y is a better predictor than x . NSE is more challenging to use directly as a loss function since it would require the dataloader to also provide the mean of the data for a given site or ecosystem type. We therefore use mean squared error (MSE) as a loss function and report its root (RMSE) as well as NSE in our results, and encourage future researchers to do the same.

Data balance in results reporting is also a concern. At first glance, the data appears very imbalanced with respect to ecosystem prevalence. CarbonSense contains 62 grassland sites, but only 1 deciduous needleleaf forest site. While this is an extreme gap, ecosystems are more diverse than IGBP taxonomies can capture; grasslands in central North America will differ significantly from those in

Europe or Asia. Still, it is prudent to separate results by ecosystem type to give a better picture of model performance.

5.5 Results

EcoPerceiver consistently outperformed the XGBoost baseline across most ecosystem types as shown in Table 2. In the low-shot regime, EcoPerceiver performed better in CVM and SNO ecosystems, but worse in DNF and WAT. In sites with greater train set prevalence EcoPerceiver scored better in all except permanent wetlands (WET)².

Our results also underline the importance of using NSE as the main metric for evaluation. Consider the models’ performance on open shrublands (OSH). XGBoost had an RMSE of 2.2995 versus EcoPerceiver’s 1.6860. The magnitude of difference is small, and both values are significantly lower than the RMSE of many other ecosystem types. But XGBoost has an NSE of -0.0945 indicating it is worse than simply guessing the mean, as opposed to EcoPerceiver achieving 0.4117. Ecosystems may have wildly different variances in their carbon fluxes, and NSE accounts for this by dividing the performance by the variance of the target.

Table 2: NSE and RMSE for each model, by IGBP ecosystem type

IGBP	XGBoost		EcoPerceiver	
	NSE	RMSE	NSE	RMSE
CRO	0.5685	4.4995	0.7009	3.7461
CSH	0.5671	2.3625	0.6253	2.1980
CVM	0.5397	2.9535	0.7029	2.3728
DBF	0.7084	3.9390	0.7820	3.4056
DNF	0.3158	3.7062	0.1745	4.0710
EBF	0.6319	5.1209	0.6451	5.0286
ENF	0.7078	3.0073	0.7156	2.9667
GRA	0.6610	2.8464	0.7229	2.5731
MF	0.6931	4.5301	0.7237	4.2984
OSH	-0.0945	2.2995	0.4117	1.6860
SAV	0.7305	2.1478	0.7909	1.8916
SNO	-1.4167	1.8208	-0.1228	1.2411
WAT	-23.7044	3.6076	-46.1290	4.9829
WET	0.5540	1.7064	0.3356	2.0828
WSA	0.4175	2.7485	0.4448	2.6832

6 Conclusion

Our work establishes a foothold for deep learning in the field of DCFM. We provide an open source ML-ready dataset, CarbonSense, using EC station data and geospatial data from a variety of ecosystems. DCFM is an inherently a time-dependent and multimodal task, and our baseline model EcoPerceiver demonstrates that recent advances in deep learning can unlock substantial performance gains in this domain. We implore more deep learning researchers to help develop this field further, because the potential of artificial intelligence to improve our world can only be realized if we actively apply it to solve pressing social and environmental issues.

Limitations Data diversity remains the biggest challenge in this domain. CarbonSense has a data imbalance in not only ecosystem types, but geographic location. Africa, Central Asia, and South America are all underrepresented. While these areas contain many EC stations, most do not have readily available data in ONEFlux format, presenting a barrier to their inclusion. Researchers should be aware of the consequences of developing models with imbalanced data, including poor performance in underrepresented areas.

²Many wetlands in CarbonSense are in the arctic-boreal region and are notoriously challenging to model due to their complex processes [6]. Inclusion of more data could potentially tip the scales.

References

- [1] C. Seiler, J. Melton, V. Arora, *et al.*, “Are terrestrial biosphere models fit for simulating the global land carbon sink?” *Journal of Advances in Modeling Earth Systems*, vol. 14, 2021. DOI: 10.1029/2021MS002946.
- [2] D. Baldocchi, K. Novick, T. Keenan, and M. Torn, “Ameriflux: Its impact on our understanding of the ‘breathing of the biosphere’, after 25 years,” *Agricultural and Forest Meteorology*, vol. 348, p. 109 929, 2024, ISSN: 0168-1923. DOI: <https://doi.org/10.1016/j.agrformet.2024.109929>. [Online]. Available: <https://www.sciencedirect.com/science/article/pii/S0168192324000443>.
- [3] A. Anav, P. Friedlingstein, M. Kidston, *et al.*, “Evaluating the land and ocean components of the global carbon cycle in the cmip5 earth system models,” *Journal of Climate*, vol. 26, no. 18, pp. 6801–6843, 2013. DOI: 10.1175/JCLI-D-12-00417.1. [Online]. Available: <https://journals.ametsoc.org/view/journals/clim/26/18/jcli-d-12-00417.1.xml>.
- [4] O. Peltola, T. Vesala, Y. Gao, *et al.*, “Monthly gridded data product of northern wetland methane emissions based on upscaling eddy covariance observations,” *Earth System Science Data*, vol. 11, no. 3, pp. 1263–1289, 2019. DOI: 10.5194/essd-11-1263-2019. [Online]. Available: <https://essd.copernicus.org/articles/11/1263/2019/>.
- [5] G. McNicol, E. Fluet-Chouinard, Z. Ouyang, *et al.*, “Upscaling wetland methane emissions from the fluxnet-ch4 eddy covariance network (upch4 v1.0): Model development, network assessment, and budget comparison,” *AGU Advances*, vol. 4, no. 5, e2023AV000956, 2023, e2023AV000956 2023AV000956. DOI: <https://doi.org/10.1029/2023AV000956>. eprint: <https://agupubs.onlinelibrary.wiley.com/doi/pdf/10.1029/2023AV000956>. [Online]. Available: <https://agupubs.onlinelibrary.wiley.com/doi/abs/10.1029/2023AV000956>.
- [6] A.-M. Virkkala, B. M. Rogers, J. D. Watts, *et al.*, “An increasing arctic-boreal co2 sink despite strong regional sources,” *bioRxiv*, 2024. DOI: 10.1101/2024.02.09.579581. [Online]. Available: <https://www.biorxiv.org/content/early/2024/02/12/2024.02.09.579581>.
- [7] J. A. Nelson, S. Walther, F. Gans, *et al.*, “X-base: The first terrestrial carbon and water flux products from an extended data-driven scaling framework, fluxcom-x,” *EGUsphere*, vol. 2024, pp. 1–51, 2024. DOI: 10.5194/egusphere-2024-165. [Online]. Available: <https://egusphere.copernicus.org/preprints/2024/egusphere-2024-165/>.
- [8] A.-M. Virkkala, J. Aalto, B. M. Rogers, *et al.*, “Statistical upscaling of ecosystem co2 fluxes across the terrestrial tundra and boreal domain: Regional patterns and uncertainties,” *Global Change Biology*, vol. 27, no. 17, pp. 4040–4059, 2021. DOI: <https://doi.org/10.1111/gcb.15659>. [Online]. Available: <https://onlinelibrary.wiley.com/doi/abs/10.1111/gcb.15659>.
- [9] C. Zhang, D. Brodylo, M. Rahman, M. A. Rahman, T. A. Douglas, and X. Comas, “Using an object-based machine learning ensemble approach to upscale evapotranspiration measured from eddy covariance towers in a subtropical wetland,” *Science of The Total Environment*, vol. 831, p. 154 969, 2022, ISSN: 0048-9697. DOI: <https://doi.org/10.1016/j.scitotenv.2022.154969>. [Online]. Available: <https://www.sciencedirect.com/science/article/pii/S0048969722020629>.
- [10] P. Xu, X. Zhu, and D. A. Clifton, “Multimodal learning with transformers: A survey,” *IEEE Transactions on Pattern Analysis and Machine Intelligence*, vol. 45, no. 10, pp. 12 113–12 132, 2023. DOI: 10.1109/TPAMI.2023.3275156.
- [11] H.-Y. Zhou, Y. Yu, C. Wang, *et al.*, “A transformer-based representation-learning model with unified processing of multimodal input for clinical diagnostics,” *Nature Biomedical Engineering*, vol. 7, no. 6, pp. 743–755, Jun. 2023, ISSN: 2157-846X. DOI: 10.1038/s41551-023-01045-x. [Online]. Available: <https://doi.org/10.1038/s41551-023-01045-x>.

- [12] J. Yao, B. Zhang, C. Li, D. Hong, and J. Chanussot, "Extended vision transformer (exvit) for land use and land cover classification: A multimodal deep learning framework," *IEEE Transactions on Geoscience and Remote Sensing*, vol. 61, pp. 1–15, 2023. DOI: 10.1109/TGRS.2023.3284671.
- [13] M. Alipour, I. La Puma, J. Picotte, *et al.*, "A multimodal data fusion and deep learning framework for large-scale wildfire surface fuel mapping," *Fire*, vol. 6, no. 2, 2023, ISSN: 2571-6255. DOI: 10.3390/fire6020036. [Online]. Available: <https://www.mdpi.com/2571-6255/6/2/36>.
- [14] D. D. Baldocchi, "How eddy covariance flux measurements have contributed to our understanding of global change biology," *Global Change Biology*, vol. 26, no. 1, pp. 242–260, 2020. DOI: <https://doi.org/10.1111/gcb.14807>. [Online]. Available: <https://onlinelibrary.wiley.com/doi/abs/10.1111/gcb.14807>.
- [15] M. Khalil, A. AlSayed, Y. Liu, and P. A. Vanrolleghem, "Machine learning for modeling n2o emissions from wastewater treatment plants: Aligning model performance, complexity, and interpretability," *Water Research*, vol. 245, p. 120667, 2023, ISSN: 0043-1354. DOI: <https://doi.org/10.1016/j.watres.2023.120667>. [Online]. Available: <https://www.sciencedirect.com/science/article/pii/S0043135423011077>.
- [16] G. Pastorello, C. Trotta, E. Canfora, *et al.*, "The FLUXNET2015 dataset and the ONEFlux processing pipeline for eddy covariance data," *Scientific Data*, vol. 7, no. 1, p. 225, Jul. 2020, ISSN: 2052-4463. DOI: 10.1038/s41597-020-0534-3. [Online]. Available: <https://doi.org/10.1038/s41597-020-0534-3>.
- [17] H. Hersbach, B. Bell, P. Berrisford, *et al.*, "The era5 global reanalysis," *Quarterly Journal of the Royal Meteorological Society*, vol. 146, no. 730, pp. 1999–2049, 2020. DOI: <https://doi.org/10.1002/qj.3803>. eprint: <https://rmets.onlinelibrary.wiley.com/doi/pdf/10.1002/qj.3803>. [Online]. Available: <https://rmets.onlinelibrary.wiley.com/doi/abs/10.1002/qj.3803>.
- [18] S. Walther, S. Besnard, J. A. Nelson, *et al.*, "Technical note: A view from space on global flux towers by modis and landsat: The fluxneteo data set," *Biogeosciences*, vol. 19, no. 11, pp. 2805–2840, 2022. DOI: 10.5194/bg-19-2805-2022. [Online]. Available: <https://bg.copernicus.org/articles/19/2805/2022/>.
- [19] C. Schaaf and Z. Wang, "MCD43A4 MODIS/Terra+Aqua BRDF/Albedo Nadir BRDF Adjusted Ref Daily L3 Global - 500m V006," 2015b. [Online]. Available: <https://www.umb.edu/spectralmass/v006/mcd43a4-nbar-product/>.
- [20] C. Schaaf and Z. Wang, "MCD43A2 MODIS/Terra+Aqua BRDF/Albedo Quality Daily L3 Global - 500m V006," 2015a. [Online]. Available: <https://www.umb.edu/spectralmass/v006/mcd43a2-albedo-product/>.
- [21] D. Sulla-Menashe and M. A. Friedl, "User Guide to Collection 6 MODIS Land Cover (MCD12Q1 and MCD12C1) Product," May 2018. [Online]. Available: <https://www.umb.edu/spectralmass/v006/mcd43a4-nbar-product/>.
- [22] ICOS RI, F. Apadula, S. Arnold, *et al.*, "ICOS Atmosphere Release 2023-1 of Level 2 Greenhouse Gas Mole Fractions of CO₂, CH₄, N₂O, CO, meteorology and 14CO₂, and flask samples analysed for CO₂, CH₄, N₂O, CO, H₂ and SF₆," 2023. DOI: <https://doi.org/10.18160/VXCS-95EV>. [Online]. Available: <https://www.icos-cp.eu/data-products/atmosphere-release>.
- [23] Warm Winter 2020 Team and ICOS Ecosystem Thematic Centre, "Warm Winter 2020 ecosystem eddy covariance flux product for 73 stations in FLUXNET-Archive format—release 2022-1 (Version 1.0).," *ICOS Carbon Portal*, 2022. DOI: 10.18160/VXCS-95EV. [Online]. Available: <https://www.icos-cp.eu/data-products/2G60-ZHAK>.
- [24] H. Chu, D. S. Christianson, Y.-W. Cheah, *et al.*, "Ameriflux base data pipeline to support network growth and data sharing," *Scientific Data*, vol. 10, no. 1, p. 614, Sep. 2023, ISSN: 2052-4463. DOI: 10.1038/s41597-023-02531-2. [Online]. Available: <https://doi.org/10.1038/s41597-023-02531-2>.

- [25] N. Gorelick, M. Hancher, M. Dixon, S. Ilyushchenko, D. Thau, and R. Moore, "Google earth engine: Planetary-scale geospatial analysis for everyone," *Remote Sensing of Environment*, 2017. DOI: 10.1016/j.rse.2017.06.031. [Online]. Available: <https://doi.org/10.1016/j.rse.2017.06.031>.
- [26] A. Jaegle, F. Gimeno, A. Brock, O. Vinyals, A. Zisserman, and J. Carreira, "Perceiver: General perception with iterative attention," in *Proceedings of the 38th International Conference on Machine Learning*, vol. 139, 18–24 Jul 2021, pp. 4651–4664.
- [27] B. Mildenhall, P. P. Srinivasan, M. Tancik, J. T. Barron, R. Ramamoorthi, and R. Ng, "Nerf: Representing scenes as neural radiance fields for view synthesis," in *ECCV*, 2020.
- [28] Z. Liu, Y. Lin, Y. Cao, *et al.*, "Swin transformer: Hierarchical vision transformer using shifted windows," in *Proceedings of the IEEE/CVF international conference on computer vision*, 2021, pp. 10 012–10 022.
- [29] R. Agarwal, M. Schwarzer, P. S. Castro, A. C. Courville, and M. Bellemare, "Deep reinforcement learning at the edge of the statistical precipice," *Advances in Neural Information Processing Systems*, vol. 34, 2021.
- [30] I. Loshchilov and F. Hutter, "Decoupled weight decay regularization," in *7th International Conference on Learning Representations, (ICLR) 2019, New Orleans, LA, USA, May 6-9, 2019*, OpenReview.net, 2019. [Online]. Available: <https://openreview.net/forum?id=Bkg6RiCqY7>.
- [31] R. McCuen, Z. Knight, and A. Cutter, "Evaluation of the nash–sutcliffe efficiency index," *Journal of Hydrologic Engineering - J HYDROL ENG*, vol. 11, Nov. 2006. DOI: 10.1061/(ASCE)1084-0699(2006)11:6(597).
- [32] C. Wagner-Riddle, "AmeriFlux FLUXNET-1F CA-ER1 Elora Research Station, Ver. 3-5," *AmeriFlux AMP*, 2021. DOI: <http://doi.org/10.17190/AMF/1832154>.
- [33] B. Amiro, "AmeriFlux FLUXNET-1F CA-MA1 Manitoba Agricultural Site 1, Ver. 3-5," *AmeriFlux AMP*, 2023. DOI: <http://doi.org/10.17190/AMF/2007165>.
- [34] B. Amiro, "AmeriFlux FLUXNET-1F CA-MA2 Manitoba Agricultural Site 2, Ver. 3-5," *AmeriFlux AMP*, 2023. DOI: <http://doi.org/10.17190/AMF/2007166>.
- [35] D. Billesbach, L. Kueppers, M. Torn, and S. Biraud, "AmeriFlux FLUXNET-1F US-A74 ARM SGP milo field, Ver. 3-5," *AmeriFlux AMP*, 2023. DOI: <http://doi.org/10.17190/AMF/2006963>.
- [36] S. Biraud, M. Fischer, S. Chan, and M. Torn, "AmeriFlux FLUXNET-1F US-ARM ARM Southern Great Plains site- Lamont, Ver. 3-5," *AmeriFlux AMP*, 2022. DOI: <http://doi.org/10.17190/AMF/1854366>.
- [37] C. Rey-Sanchez, C. T. Wang, D. Szutu, *et al.*, "AmeriFlux FLUXNET-1F US-Bi1 Bouldin Island Alfalfa, Ver. 3-5," *AmeriFlux AMP*, 2022. DOI: <http://doi.org/10.17190/AMF/1871134>.
- [38] C. Rey-Sanchez, C. T. Wang, D. Szutu, K. Hemes, J. Verfaillie, and D. Baldocchi, "AmeriFlux FLUXNET-1F US-Bi2 Bouldin Island corn, Ver. 3-5," *AmeriFlux AMP*, 2022. DOI: <http://doi.org/10.17190/AMF/1871135>.
- [39] C. L. Phillips and D. Huggins, "AmeriFlux FLUXNET-1F US-CF1 CAF-LTAR Cook East, Ver. 3-5," *AmeriFlux AMP*, 2021. DOI: <http://doi.org/10.17190/AMF/1832158>.
- [40] D. Huggins, "AmeriFlux FLUXNET-1F US-CF2 CAF-LTAR Cook West, Ver. 3-5," *AmeriFlux AMP*, 2022. DOI: <http://doi.org/10.17190/AMF/1881573>.
- [41] D. Huggins, "AmeriFlux FLUXNET-1F US-CF3 CAF-LTAR Boyd North, Ver. 3-5," *AmeriFlux AMP*, 2022. DOI: <http://doi.org/10.17190/AMF/1881574>.
- [42] D. Huggins, "AmeriFlux FLUXNET-1F US-CF4 CAF-LTAR Boyd South, Ver. 3-5," *AmeriFlux AMP*, 2022. DOI: <http://doi.org/10.17190/AMF/1881575>.
- [43] J. Chen and H. Chu, "AmeriFlux FLUXNET-1F US-CRT Curtice Walter-Berger cropland, Ver. 3-5," *AmeriFlux AMP*, 2023. DOI: <http://doi.org/10.17190/AMF/2006974>.

- 464 [44] A. Desai, “AmeriFlux FLUXNET-1F US-CS1 Central Sands Irrigated Agricultural Field, Ver.
465 3-5,” *AmeriFlux AMP*, 2022. DOI: <http://doi.org/10.17190/AMF/1881576>.
- 466 [45] A. Desai, “AmeriFlux FLUXNET-1F US-CS3 Central Sands Irrigated Agricultural Field, Ver.
467 3-5,” *AmeriFlux AMP*, 2022. DOI: <http://doi.org/10.17190/AMF/1881578>.
- 468 [46] A. Desai, “AmeriFlux FLUXNET-1F US-CS4 Central Sands Irrigated Agricultural Field, Ver.
469 3-5,” *AmeriFlux AMP*, 2022. DOI: <http://doi.org/10.17190/AMF/1881579>.
- 470 [47] A. Duff and A. Desai, “AmeriFlux FLUXNET-1F US-DFC US Dairy Forage Research Center,
471 Prairie du Sac, Ver. 3-5,” *AmeriFlux AMP*, 2023. DOI: <http://doi.org/10.17190/AMF/2006975>.
- 472 [48] M. R. Schuppenhauer, S. C. Biraud, S. Deverel, and S. Chan, “AmeriFlux FLUXNET-1F
473 US-DS3 Staten Rice 1, Ver. 3-5,” *AmeriFlux AMP*, 2023. DOI: <http://doi.org/10.17190/AMF/2229376>.
- 474 [49] S. Fares, “AmeriFlux FLUXNET-1F US-Lin Lindcove Orange Orchard, Ver. 3-5,” *AmeriFlux*
475 *AMP*, 2023. DOI: <http://doi.org/10.17190/AMF/2229381>.
- 476 [50] A. Schreiner-McGraw, “AmeriFlux FLUXNET-1F US-Mo1 LTAR CMRB Field 1 (CMRB
477 ASP), Ver. 3-5,” *AmeriFlux AMP*, 2023. DOI: <http://doi.org/10.17190/AMF/2229382>.
- 478 [51] A. Schreiner-McGraw, “AmeriFlux FLUXNET-1F US-Mo3 LTAR CMRB Field 3 (CMRB
479 BAU), Ver. 3-5,” *AmeriFlux AMP*, 2023. DOI: <http://doi.org/10.17190/AMF/2229384>.
- 480 [52] A. Suyker, “AmeriFlux FLUXNET-1F US-Ne1 Mead - irrigated continuous maize site, Ver.
481 3-5,” *AmeriFlux AMP*, 2022. DOI: <http://doi.org/10.17190/AMF/1871140>.
- 482 [53] M. R. Schuppenhauer, S. C. Biraud, and S. Chan, “AmeriFlux FLUXNET-1F US-RGA
483 Arkansas Corn Farm, Ver. 3-5,” *AmeriFlux AMP*, 2023. DOI: <http://doi.org/10.17190/AMF/2204873>.
- 484 [54] M. Schuppenhauer, S. C. Biraud, and S. Chan, “AmeriFlux FLUXNET-1F US-RGB Butte
485 County Rice Farm, Ver. 3-5,” *AmeriFlux AMP*, 2023. DOI: <http://doi.org/10.17190/AMF/2204874>.
- 486 [55] M. R. Schuppenhauer, S. C. Biraud, and S. Chan, “AmeriFlux FLUXNET-1F US-RGo Glenn
487 County Organic Rice Farm, Ver. 3-5,” *AmeriFlux AMP*, 2023. DOI: <http://doi.org/10.17190/AMF/2204875>.
- 488 [56] J. Baker, T. Griffis, and T. Griffis, “AmeriFlux FLUXNET-1F US-Ro1 Rosemount- G21, Ver.
489 3-5,” *AmeriFlux AMP*, 2022. DOI: <http://doi.org/10.17190/AMF/1881588>.
- 490 [57] J. Baker and T. Griffis, “AmeriFlux FLUXNET-1F US-Ro2 Rosemount- C7, Ver. 3-5,”
491 *AmeriFlux AMP*, 2023. DOI: <http://doi.org/10.17190/AMF/2204876>.
- 492 [58] J. Baker and T. Griffis, “AmeriFlux FLUXNET-1F US-Ro5 Rosemount I18_{South}, Ver.3–5,”
493 *AmeriFlux AMP*, 2021. DOI: <http://doi.org/10.17190/AMF/1818371>.
- 494 [59] J. Baker and T. Griffis, “AmeriFlux FLUXNET-1F US-Ro6 Rosemount I18_{North}, Ver.3–5,”
495 *AmeriFlux AMP*, 2022. DOI: <http://doi.org/10.17190/AMF/1881590>.
- 496 [60] C. Sturtevant, J. Verfaillie, and D. Baldocchi, “AmeriFlux FLUXNET-1F US-Tw2 Twitchell
497 Corn, Ver. 3-5,” *AmeriFlux AMP*, 2022. DOI: <http://doi.org/10.17190/AMF/1881593>.
- 498 [61] S. D. Chamberlain, P. Oikawa, C. Sturtevant, D. Szutu, J. Verfaillie, and D. Baldocchi,
499 “AmeriFlux FLUXNET-1F US-Tw3 Twitchell Alfalfa, Ver. 3-5,” *AmeriFlux AMP*, 2022. DOI:
500 <http://doi.org/10.17190/AMF/1881594>.
- 501 [62] N. (E. O. Network), “AmeriFlux FLUXNET-1F US-xSL NEON North Sterling, CO (STER),
502 Ver. 3-5,” *AmeriFlux AMP*, 2023. DOI: <http://doi.org/10.17190/AMF/2229411>.
- 503 [63] B. Drake, R. Hinkle, R. Bracho, S. Dore, and T. Powell, “AmeriFlux FLUXNET-1F US-
504 KS2 Kennedy Space Center (scrub oak), Ver. 3-5,” *AmeriFlux AMP*, 2023. DOI: <http://doi.org/10.17190/AMF/2229380>.
- 505 [64] G. Flerchinger, “AmeriFlux FLUXNET-1F US-Rls RCEW Low Sagebrush, Ver. 3-5,” *Ameri-
506 Flux AMP*, 2023. DOI: <http://doi.org/10.17190/AMF/2229387>.
- 507 [65] G. Flerchinger, “AmeriFlux FLUXNET-1F US-Rms RCEW Mountain Big Sagebrush, Ver.
508 3-5,” *AmeriFlux AMP*, 2022. DOI: <http://doi.org/10.17190/AMF/1881587>.

- [66] G. Flerchinger and M. L. Reba, “AmeriFlux FLUXNET-1F US-Rwe RCEW Reynolds Mountain East, Ver. 3-5,” *AmeriFlux AMP*, 2022. DOI: <http://doi.org/10.17190/AMF/1871143>.
- [67] G. Flerchinger, “AmeriFlux FLUXNET-1F US-Rwf RCEW Upper Sheep Prescribed Fire, Ver. 3-5,” *AmeriFlux AMP*, 2022. DOI: <http://doi.org/10.17190/AMF/1881591>.
- [68] S. Goslee, “AmeriFlux FLUXNET-1F US-HWB USDA ARS Pasture Sytems and Watershed Management Research Unit- Hawbecker Site, Ver. 3-5,” *AmeriFlux AMP*, 2022. DOI: <http://doi.org/10.17190/AMF/1881582>.
- [69] N. (E. O. Network), “AmeriFlux FLUXNET-1F US-xDS NEON Disney Wilderness Preserve (DSNY), Ver. 3-5,” *AmeriFlux AMP*, 2023. DOI: <http://doi.org/10.17190/AMF/1985439>.
- [70] R. Staebler, “AmeriFlux FLUXNET-1F CA-Cbo Ontario - Mixed Deciduous, Borden Forest Site, Ver. 3-5,” *AmeriFlux AMP*, 2022. DOI: <http://doi.org/10.17190/AMF/1854365>.
- [71] M. A. Arain, “AmeriFlux FLUXNET-1F CA-TPD Ontario - Turkey Point Mature Deciduous, Ver. 3-5,” *AmeriFlux AMP*, 2022. DOI: <http://doi.org/10.17190/AMF/1881567>.
- [72] E. A. Yopez and J. Garatuza, “AmeriFlux FLUXNET-1F MX-Tes Tesopaco, secondary tropical dry forest, Ver. 3-5,” *AmeriFlux AMP*, 2021. DOI: <http://doi.org/10.17190/AMF/1832156>.
- [73] A. Richardson and D. Hollinger, “AmeriFlux FLUXNET-1F US-Bar Bartlett Experimental Forest, Ver. 3-5,” *AmeriFlux AMP*, 2023. DOI: <http://doi.org/10.17190/AMF/2006969>.
- [74] J. W. Munger, “AmeriFlux FLUXNET-1F US-Ha1 Harvard Forest EMS Tower (HFR1), Ver. 3-5,” *AmeriFlux AMP*, 2022. DOI: <http://doi.org/10.17190/AMF/1871137>.
- [75] K. Novick and R. Phillips, “AmeriFlux FLUXNET-1F US-MMS Morgan Monroe State Forest, Ver. 3-5,” *AmeriFlux AMP*, 2022. DOI: <http://doi.org/10.17190/AMF/1854369>.
- [76] J. Wood and L. Gu, “AmeriFlux FLUXNET-1F US-MOz Missouri Ozark Site, Ver. 3-5,” *AmeriFlux AMP*, 2021. DOI: <http://doi.org/10.17190/AMF/1854370>.
- [77] J. Chen, H. Chu, and A. Noormets, “AmeriFlux FLUXNET-1F US-Oho Oak Openings, Ver. 3-5,” *AmeriFlux AMP*, 2023. DOI: <http://doi.org/10.17190/AMF/2229385>.
- [78] M. Ueyama, H. Iwata, and Y. Harazono, “AmeriFlux FLUXNET-1F US-Rpf Poker Flat Research Range: Succession from fire scar to deciduous forest, Ver. 3-5,” *AmeriFlux AMP*, 2023. DOI: <http://doi.org/10.17190/AMF/2229388>.
- [79] C. Gough, G. Bohrer, and P. Curtis, “AmeriFlux FLUXNET-1F US-UMB Univ. of Mich. Biological Station, Ver. 3-5,” *AmeriFlux AMP*, 2023. DOI: <http://doi.org/10.17190/AMF/2204882>.
- [80] C. Gough, G. Bohrer, and P. Curtis, “AmeriFlux FLUXNET-1F US-UMd UMBS Disturbance, Ver. 3-5,” *AmeriFlux AMP*, 2022. DOI: <http://doi.org/10.17190/AMF/1881597>.
- [81] J. Chen, “AmeriFlux FLUXNET-1F US-Wi1 Intermediate hardwood (IHW), Ver. 3-5,” *AmeriFlux AMP*, 2023. DOI: <http://doi.org/10.17190/AMF/2229394>.
- [82] J. Chen, “AmeriFlux FLUXNET-1F US-Wi3 Mature hardwood (MHW), Ver. 3-5,” *AmeriFlux AMP*, 2023. DOI: <http://doi.org/10.17190/AMF/2229395>.
- [83] J. Chen, “AmeriFlux FLUXNET-1F US-Wi8 Young hardwood clearcut (YHW), Ver. 3-5,” *AmeriFlux AMP*, 2023. DOI: <http://doi.org/10.17190/AMF/2229400>.
- [84] N. (E. O. Network), “AmeriFlux FLUXNET-1F US-xBL NEON Blandy Experimental Farm (BLAN), Ver. 3-5,” *AmeriFlux AMP*, 2023. DOI: <http://doi.org/10.17190/AMF/2229405>.
- [85] N. (E. O. Network), “AmeriFlux FLUXNET-1F US-xBR NEON Bartlett Experimental Forest (BART), Ver. 3-5,” *AmeriFlux AMP*, 2022. DOI: <http://doi.org/10.17190/AMF/1881598>.
- [86] N. (E. O. Network), “AmeriFlux FLUXNET-1F US-xGR NEON Great Smoky Mountains National Park, Twin Creeks (GRSM), Ver. 3-5,” *AmeriFlux AMP*, 2023. DOI: <http://doi.org/10.17190/AMF/1985440>.

- 566 [87] N. (E. O. Network), “AmeriFlux FLUXNET-1F US-xHA NEON Harvard Forest (HARV),
567 Ver. 3-5,” *AmeriFlux AMP*, 2023. DOI: <http://doi.org/10.17190/AMF/1985441>.
- 568 [88] N. (E. O. Network), “AmeriFlux FLUXNET-1F US-xML NEON Mountain Lake Biological
569 Station (MLBS), Ver. 3-5,” *AmeriFlux AMP*, 2023. DOI: <http://doi.org/10.17190/AMF/1985447>.
- 570
571 [89] N. (E. O. Network), “AmeriFlux FLUXNET-1F US-xSC NEON Smithsonian Conservation
572 Biology Institute (SCBI), Ver. 3-5,” *AmeriFlux AMP*, 2023. DOI: <http://doi.org/10.17190/AMF/2229409>.
- 573
574 [90] N. (E. O. Network), “AmeriFlux FLUXNET-1F US-xSE NEON Smithsonian Environmental
575 Research Center (SERC), Ver. 3-5,” *AmeriFlux AMP*, 2023. DOI: <http://doi.org/10.17190/AMF/1985452>.
- 576
577 [91] N. (E. O. Network), “AmeriFlux FLUXNET-1F US-xST NEON Steigerwaldt Land Services
578 (STEI), Ver. 3-5,” *AmeriFlux AMP*, 2023. DOI: <http://doi.org/10.17190/AMF/1985454>.
- 579
580 [92] N. (E. O. Network), “AmeriFlux FLUXNET-1F US-xTR NEON Treehaven (TREE), Ver.
581 3-5,” *AmeriFlux AMP*, 2023. DOI: <http://doi.org/10.17190/AMF/1985456>.
- 582 [93] N. (E. O. Network), “AmeriFlux FLUXNET-1F US-xUK NEON The University of Kansas
583 Field Station (UKFS), Ver. 3-5,” *AmeriFlux AMP*, 2023. DOI: <http://doi.org/10.17190/AMF/1985457>.
- 584
585 [94] A. Antonino, “AmeriFlux FLUXNET-1F BR-CST Caatinga Serra Talhada, Ver. 3-5,” *Ameri-
586 Flux AMP*, 2022. DOI: <http://doi.org/10.17190/AMF/1902820>.
- 587 [95] T. A. Black, “AmeriFlux FLUXNET-1F CA-Ca1 British Columbia - 1949 Douglas-fir stand,
588 Ver. 3-5,” *AmeriFlux AMP*, 2023. DOI: <http://doi.org/10.17190/AMF/2007163>.
- 589 [96] T. A. Black, “AmeriFlux FLUXNET-1F CA-Ca2 British Columbia - Clearcut Douglas-fir
590 stand (harvested winter 1999/2000), Ver. 3-5,” *AmeriFlux AMP*, 2023. DOI: <http://doi.org/10.17190/AMF/2007164>.
- 591
592 [97] T. A. Black, “AmeriFlux FLUXNET-1F CA-LP1 British Columbia - Mountain pine beetle-
593 attacked lodgepole pine stand , Ver. 3-5,” *AmeriFlux AMP*, 2021. DOI: <http://doi.org/10.17190/AMF/1832155>.
- 594
595 [98] M. Goulden, “AmeriFlux FLUXNET-1F CA-NS1 UCI-1850 burn site, Ver. 3-5,” *AmeriFlux
596 AMP*, 2022. DOI: <http://doi.org/10.17190/AMF/1902824>.
- 597 [99] M. Goulden, “AmeriFlux FLUXNET-1F CA-NS2 UCI-1930 burn site, Ver. 3-5,” *AmeriFlux
598 AMP*, 2022. DOI: <http://doi.org/10.17190/AMF/1902825>.
- 599 [100] M. Goulden, “AmeriFlux FLUXNET-1F CA-NS3 UCI-1964 burn site, Ver. 3-5,” *AmeriFlux
600 AMP*, 2022. DOI: <http://doi.org/10.17190/AMF/1902826>.
- 601 [101] M. Goulden, “AmeriFlux FLUXNET-1F CA-NS4 UCI-1964 burn site wet, Ver. 3-5,” *Ameri-
602 Flux AMP*, 2022. DOI: <http://doi.org/10.17190/AMF/1902827>.
- 603 [102] M. Goulden, “AmeriFlux FLUXNET-1F CA-NS5 UCI-1981 burn site, Ver. 3-5,” *AmeriFlux
604 AMP*, 2022. DOI: <http://doi.org/10.17190/AMF/1902828>.
- 605 [103] H. A. Margolis, “AmeriFlux FLUXNET-1F CA-Qfo Quebec - Eastern Boreal, Mature Black
606 Spruce, Ver. 3-5,” *AmeriFlux AMP*, 2023. DOI: <http://doi.org/10.17190/AMF/2006960>.
- 607
608 [104] B. Amiro, “AmeriFlux FLUXNET-1F CA-SF1 Saskatchewan - Western Boreal, forest burned
609 in 1977, Ver. 3-5,” *AmeriFlux AMP*, 2022. DOI: <http://doi.org/10.17190/AMF/1902831>.
- 610
611 [105] B. Amiro, “AmeriFlux FLUXNET-1F CA-SF2 Saskatchewan - Western Boreal, forest burned
612 in 1989, Ver. 3-5,” *AmeriFlux AMP*, 2023. DOI: <http://doi.org/10.17190/AMF/2006961>.
- 613
614 [106] M. A. Arain, “AmeriFlux FLUXNET-1F CA-TP1 Ontario - Turkey Point 2002 Plantation
615 White Pine, Ver. 3-5,” *AmeriFlux AMP*, 2023. DOI: <http://doi.org/10.17190/AMF/2006962>.
- 616

- 617 [107] M. A. Arain, “AmeriFlux FLUXNET-1F CA-TP3 Ontario - Turkey Point 1974 Plantation
618 White Pine, Ver. 3-5,” *AmeriFlux AMP*, 2022. DOI: [http://doi.org/10.17190/AMF/](http://doi.org/10.17190/AMF/1881566)
619 1881566.
- 620 [108] E. Euskirchen, “AmeriFlux FLUXNET-1F US-BZS Bonanza Creek Black Spruce, Ver. 3-5,”
621 *AmeriFlux AMP*, 2022. DOI: <http://doi.org/10.17190/AMF/1881572>.
- 622 [109] A. Desai, “AmeriFlux FLUXNET-1F US-CS2 Tri county school Pine Forest, Ver. 3-5,”
623 *AmeriFlux AMP*, 2022. DOI: <http://doi.org/10.17190/AMF/1881577>.
- 624 [110] S. Dore and T. Kolb, “AmeriFlux FLUXNET-1F US-Fmf Flagstaff - Managed Forest, Ver.
625 3-5,” *AmeriFlux AMP*, 2023. DOI: <http://doi.org/10.17190/AMF/2007173>.
- 626 [111] S. Dore and T. Kolb, “AmeriFlux FLUXNET-1F US-Fuf Flagstaff - Unmanaged Forest, Ver.
627 3-5,” *AmeriFlux AMP*, 2023. DOI: <http://doi.org/10.17190/AMF/2007174>.
- 628 [112] J. Frank and B. Massman, “AmeriFlux FLUXNET-1F US-GLE GLEES, Ver. 3-5,” *AmeriFlux*
629 *AMP*, 2022. DOI: <http://doi.org/10.17190/AMF/1871136>.
- 630 [113] J. D. Forsythe, M. A. Kline, and T. L. O’Halloran, “AmeriFlux FLUXNET-1F US-HB2
631 Hobcaw Barony Mature Longleaf Pine, Ver. 3-5,” *AmeriFlux AMP*, 2023. DOI: <http://doi.org/10.17190/AMF/2229377>.
- 632 [114] J. D. Forsythe, M. A. Kline, and T. L. O’Halloran, “AmeriFlux FLUXNET-1F US-HB3
633 Hobcaw Barony Longleaf Pine Restoration, Ver. 3-5,” *AmeriFlux AMP*, 2023. DOI: <http://doi.org/10.17190/AMF/2229378>.
- 634 [115] D. Hollinger, “AmeriFlux FLUXNET-1F US-Ho2 Howland Forest (west tower), Ver. 3-5,”
635 *AmeriFlux AMP*, 2022. DOI: <http://doi.org/10.17190/AMF/1881581>.
- 636 [116] B. Drake, R. Hinkle, R. Bracho, T. Powell, and S. Dore, “AmeriFlux FLUXNET-1F US-
637 KS1 Kennedy Space Center (slash pine), Ver. 3-5,” *AmeriFlux AMP*, 2023. DOI: <http://doi.org/10.17190/AMF/2229379>.
- 638 [117] B. Law, “AmeriFlux FLUXNET-1F US-Me1 Metolius - Eyerly burn, Ver. 3-5,” *AmeriFlux*
639 *AMP*, 2022. DOI: <http://doi.org/10.17190/AMF/1902834>.
- 640 [118] B. Law, “AmeriFlux FLUXNET-1F US-Me2 Metolius mature ponderosa pine, Ver. 3-5,”
641 *AmeriFlux AMP*, 2021. DOI: <http://doi.org/10.17190/AMF/1854368>.
- 642 [119] B. Law, “AmeriFlux FLUXNET-1F US-Me3 Metolius-second young aged pine, Ver. 3-5,”
643 *AmeriFlux AMP*, 2022. DOI: <http://doi.org/10.17190/AMF/1902835>.
- 644 [120] B. Law, “AmeriFlux FLUXNET-1F US-Me6 Metolius Young Pine Burn, Ver. 3-5,” *AmeriFlux*
645 *AMP*, 2023. DOI: <http://doi.org/10.17190/AMF/2204871>.
- 646 [121] A. Noormets, G. Sun, M. Gavazzi, S. McNulty, J.-C. Domec, and J. King, “AmeriFlux
647 FLUXNET-1F US-NC1 NC_Clearcut, Ver.3 – 5,” *AmeriFlux AMP*, 2022. DOI: <http://doi.org/10.17190/AMF/1902836>.
- 648 [122] A. Noormets, M. Gavazzi, M. Aguilos, J. King, B. Mitra, and J.-C. Domec, “AmeriFlux
649 FLUXNET-1F US-NC3 NC_Clearcut3, Ver.3 – 5,” *AmeriFlux AMP*, 2023. DOI: <http://doi.org/10.17190/AMF/2204872>.
- 650 [123] P. D. Blanken, R. K. Monson, S. P. Burns, D. R. Bowling, and A. A. Turnipseed, “AmeriFlux
651 FLUXNET-1F US-NR1 Niwot Ridge Forest (LTER NWT1), Ver. 3-5,” *AmeriFlux AMP*,
652 2022. DOI: <http://doi.org/10.17190/AMF/1871141>.
- 653 [124] M. Litvak, “AmeriFlux FLUXNET-1F US-Vcm Valles Caldera Mixed Conifer, Ver. 3-5,”
654 *AmeriFlux AMP*, 2023. DOI: <http://doi.org/10.17190/AMF/2229391>.
- 655 [125] M. Litvak, “AmeriFlux FLUXNET-1F US-Vcp Valles Caldera Ponderosa Pine, Ver. 3-5,”
656 *AmeriFlux AMP*, 2023. DOI: <http://doi.org/10.17190/AMF/2229392>.
- 657 [126] J. Chen, “AmeriFlux FLUXNET-1F US-Wi0 Young red pine (YRP), Ver. 3-5,” *AmeriFlux*
658 *AMP*, 2023. DOI: <http://doi.org/10.17190/AMF/2229393>.
- 659 [127] J. Chen, “AmeriFlux FLUXNET-1F US-Wi4 Mature red pine (MRP), Ver. 3-5,” *AmeriFlux*
660 *AMP*, 2023. DOI: <http://doi.org/10.17190/AMF/2229396>.
- 661 [128] J. Chen, “AmeriFlux FLUXNET-1F US-Wi5 Mixed young jack pine (MYJP), Ver. 3-5,”
662 *AmeriFlux AMP*, 2023. DOI: <http://doi.org/10.17190/AMF/2229397>.
- 663
664
665
666
667

- 668 [129] J. Chen, “AmeriFlux FLUXNET-1F US-Wi9 Young Jack pine (YJP), Ver. 3-5,” *AmeriFlux*
669 *AMP*, 2023. DOI: <http://doi.org/10.17190/AMF/2229401>.
- 670 [130] N. (E. O. Network), “AmeriFlux FLUXNET-1F US-xAB NEON Abby Road (ABBY), Ver.
671 3-5,” *AmeriFlux AMP*, 2023. DOI: <http://doi.org/10.17190/AMF/2229403>.
- 672 [131] N. (E. O. Network), “AmeriFlux FLUXNET-1F US-xBN NEON Caribou Creek - Poker
673 Flats Watershed (BONA), Ver. 3-5,” *AmeriFlux AMP*, 2023. DOI: <http://doi.org/10.17190/AMF/2229406>.
- 674 [132] N. (E. O. Network), “AmeriFlux FLUXNET-1F US-xDJ NEON Delta Junction (DEJU), Ver.
675 3-5,” *AmeriFlux AMP*, 2023. DOI: <http://doi.org/10.17190/AMF/2229407>.
- 676 [133] N. (E. O. Network), “AmeriFlux FLUXNET-1F US-xJE NEON Jones Ecological Research
677 Center (JERC), Ver. 3-5,” *AmeriFlux AMP*, 2023. DOI: <http://doi.org/10.17190/AMF/1985443>.
- 678 [134] N. (E. O. Network), “AmeriFlux FLUXNET-1F US-xRM NEON Rocky Mountain National
679 Park, CASTNET (RMNP), Ver. 3-5,” *AmeriFlux AMP*, 2023. DOI: <http://doi.org/10.17190/AMF/1985450>.
- 680 [135] N. (E. O. Network), “AmeriFlux FLUXNET-1F US-xSB NEON Ordway-Swisher Biological
681 Station (OSBS), Ver. 3-5,” *AmeriFlux AMP*, 2023. DOI: <http://doi.org/10.17190/AMF/1985451>.
- 682 [136] N. (E. O. Network), “AmeriFlux FLUXNET-1F US-xTA NEON Talladega National Forest
683 (TALL), Ver. 3-5,” *AmeriFlux AMP*, 2023. DOI: <http://doi.org/10.17190/AMF/1985455>.
- 684 [137] N. (E. O. Network), “AmeriFlux FLUXNET-1F US-xYE NEON Yellowstone Northern
685 Range (Frog Rock) (YELL), Ver. 3-5,” *AmeriFlux AMP*, 2023. DOI: <http://doi.org/10.17190/AMF/1985459>.
- 686 [138] B. Amiro, “AmeriFlux FLUXNET-1F CA-MA3 Manitoba Agricultural Site 3, Ver. 3-5,”
687 *AmeriFlux AMP*, 2023. DOI: <http://doi.org/10.17190/AMF/2007167>.
- 688 [139] D. Billesbach, L. Kueppers, M. Torn, and S. Biraud, “AmeriFlux FLUXNET-1F US-A32
689 ARM-SGP Medford hay pasture, Ver. 3-5,” *AmeriFlux AMP*, 2022. DOI: <http://doi.org/10.17190/AMF/1881568>.
- 690 [140] D. Billesbach, J. Bradford, and M. Torn, “AmeriFlux FLUXNET-1F US-AR1 ARM USDA
691 UNL OSU Woodward Switchgrass 1, Ver. 3-5,” *AmeriFlux AMP*, 2023. DOI: <http://doi.org/10.17190/AMF/2006965>.
- 692 [141] D. Billesbach, J. Bradford, and M. Torn, “AmeriFlux FLUXNET-1F US-AR2 ARM USDA
693 UNL OSU Woodward Switchgrass 2, Ver. 3-5,” *AmeriFlux AMP*, 2023. DOI: <http://doi.org/10.17190/AMF/2006966>.
- 694 [142] M. Torn, “AmeriFlux FLUXNET-1F US-ARb ARM Southern Great Plains burn site- Lamont,
695 Ver. 3-5,” *AmeriFlux AMP*, 2023. DOI: <http://doi.org/10.17190/AMF/2006967>.
- 696 [143] M. Torn, “AmeriFlux FLUXNET-1F US-ARc ARM Southern Great Plains control site-
697 Lamont, Ver. 3-5,” *AmeriFlux AMP*, 2023. DOI: <http://doi.org/10.17190/AMF/2006968>.
- 698 [144] K. Novick, “AmeriFlux FLUXNET-1F US-BRG Bayles Road Grassland Tower, Ver. 3-5,”
699 *AmeriFlux AMP*, 2023. DOI: <http://doi.org/10.17190/AMF/2006970>.
- 700 [145] D. Bowling, “AmeriFlux FLUXNET-1F US-Cop Corral Pocket, Ver. 3-5,” *AmeriFlux AMP*,
701 2023. DOI: <http://doi.org/10.17190/AMF/2006972>.
- 702 [146] H. Liu, M. Huang, and X. Chen, “AmeriFlux FLUXNET-1F US-Hn2 Hanford 100H grassland,
703 Ver. 3-5,” *AmeriFlux AMP*, 2022. DOI: <http://doi.org/10.17190/AMF/1902832>.
- 704 [147] N. Brunsell, “AmeriFlux FLUXNET-1F US-KFS Kansas Field Station, Ver. 3-5,” *AmeriFlux*
705 *AMP*, 2022. DOI: <http://doi.org/10.17190/AMF/1881585>.
- 706 [148] N. Brunsell, “AmeriFlux FLUXNET-1F US-KLS Kansas Land Institute, Ver. 3-5,” *AmeriFlux*
707 *AMP*, 2021. DOI: <http://doi.org/10.17190/AMF/1854367>.

- 718 [149] N. Brunsell, “AmeriFlux FLUXNET-1F US-Kon Konza Prairie LTER (KNZ), Ver. 3-5,”
719 *AmeriFlux AMP*, 2023. DOI: <http://doi.org/10.17190/AMF/2316062>.
- 720 [150] A. Schreiner-McGraw, “AmeriFlux FLUXNET-1F US-Mo2 LTAR CMRB Tucker Prairie
721 (CMRB TP), Ver. 3-5,” *AmeriFlux AMP*, 2023. DOI: <http://doi.org/10.17190/AMF/2229383>.
722
- 723 [151] M. Torn and S. Dengel, “AmeriFlux FLUXNET-1F US-NGC NGEE Arctic Council, Ver.
724 3-5,” *AmeriFlux AMP*, 2022. DOI: <http://doi.org/10.17190/AMF/1902838>.
- 725 [152] M. L. Silveira and R. Bracho, “AmeriFlux FLUXNET-1F US-ONA Florida pine flatwoods,
726 Ver. 3-5,” *AmeriFlux AMP*, 2021. DOI: <http://doi.org/10.17190/AMF/1832163>.
- 727 [153] J. Baker and T. Griffis, “AmeriFlux FLUXNET-1F US-Ro4 Rosemount Prairie, Ver. 3-5,”
728 *AmeriFlux AMP*, 2022. DOI: <http://doi.org/10.17190/AMF/1881589>.
- 729 [154] R. Scott, “AmeriFlux FLUXNET-1F US-SRG Santa Rita Grassland, Ver. 3-5,” *AmeriFlux*
730 *AMP*, 2023. DOI: <http://doi.org/10.17190/AMF/2204877>.
- 731 [155] M. Litvak, “AmeriFlux FLUXNET-1F US-Seg Seville grassland, Ver. 3-5,” *AmeriFlux*
732 *AMP*, 2023. DOI: <http://doi.org/10.17190/AMF/1984572>.
- 733 [156] R. Shortt, K. Hemes, D. Szutu, J. Verfaillie, and D. Baldocchi, “AmeriFlux FLUXNET-1F
734 US-Sne Sherman Island Restored Wetland, Ver. 3-5,” *AmeriFlux AMP*, 2022. DOI: <http://doi.org/10.17190/AMF/1871144>.
735
- 736 [157] K. Kusak, C. R. Sanchez, D. Szutu, and D. Baldocchi, “AmeriFlux FLUXNET-1F US-Snf
737 Sherman Barn, Ver. 3-5,” *AmeriFlux AMP*, 2022. DOI: <http://doi.org/10.17190/AMF/1854371>.
738
- 739 [158] S. Ma, L. Xu, J. Verfaillie, and D. Baldocchi, “AmeriFlux FLUXNET-1F US-Var Vaira Ranch-
740 Ione, Ver. 3-5,” *AmeriFlux AMP*, 2023. DOI: <http://doi.org/10.17190/AMF/1993904>.
- 741 [159] R. Scott, “AmeriFlux FLUXNET-1F US-Wkg Walnut Gulch Kendall Grasslands, Ver. 3-5,”
742 *AmeriFlux AMP*, 2023. DOI: <http://doi.org/10.17190/AMF/1984575>.
- 743 [160] N. (E. O. Network), “AmeriFlux FLUXNET-1F US-xAE NEON Klemme Range Research
744 Station (OAES), Ver. 3-5,” *AmeriFlux AMP*, 2023. DOI: <http://doi.org/10.17190/AMF/1985434>.
745
- 746 [161] N. (E. O. Network), “AmeriFlux FLUXNET-1F US-xCL NEON LBJ National Grassland
747 (CLBJ), Ver. 3-5,” *AmeriFlux AMP*, 2023. DOI: <http://doi.org/10.17190/AMF/1985435>.
748
- 749 [162] N. (E. O. Network), “AmeriFlux FLUXNET-1F US-xCP NEON Central Plains Experimental
750 Range (CPER), Ver. 3-5,” *AmeriFlux AMP*, 2023. DOI: <http://doi.org/10.17190/AMF/1985436>.
751
- 752 [163] N. (E. O. Network), “AmeriFlux FLUXNET-1F US-xDC NEON Dakota Coteau Field
753 School (DCFS), Ver. 3-5,” *AmeriFlux AMP*, 2023. DOI: <http://doi.org/10.17190/AMF/1985437>.
754
- 755 [164] N. (E. O. Network), “AmeriFlux FLUXNET-1F US-xKA NEON Konza Prairie Biological
756 Station - Relocatable (KONA), Ver. 3-5,” *AmeriFlux AMP*, 2023. DOI: <http://doi.org/10.17190/AMF/1985444>.
757
- 758 [165] N. (E. O. Network), “AmeriFlux FLUXNET-1F US-xKZ NEON Konza Prairie Biological
759 Station (KONZ), Ver. 3-5,” *AmeriFlux AMP*, 2023. DOI: <http://doi.org/10.17190/AMF/1985445>.
760
- 761 [166] N. (E. O. Network), “AmeriFlux FLUXNET-1F US-xNG NEON Northern Great Plains
762 Research Laboratory (NOGP), Ver. 3-5,” *AmeriFlux AMP*, 2023. DOI: <http://doi.org/10.17190/AMF/1985448>.
763
- 764 [167] N. (E. O. Network), “AmeriFlux FLUXNET-1F US-xWD NEON Woodworth (WOOD), Ver.
765 3-5,” *AmeriFlux AMP*, 2023. DOI: <http://doi.org/10.17190/AMF/2229412>.
- 766 [168] H. McCaughey, “AmeriFlux FLUXNET-1F CA-Gro Ontario - Groundhog River, Boreal
767 Mixedwood Forest, Ver. 3-5,” *AmeriFlux AMP*, 2022. DOI: <http://doi.org/10.17190/AMF/1902823>.
768

- 769 [169] A. Desai, “AmeriFlux FLUXNET-1F US-Syv Sylvania Wilderness Area, Ver. 3-5,” *AmeriFlux*
770 *AMP*, 2023. DOI: <http://doi.org/10.17190/AMF/2204879>.
- 771 [170] N. (E. O. Network), “AmeriFlux FLUXNET-1F US-xDL NEON Dead Lake (DELA), Ver.
772 3-5,” *AmeriFlux AMP*, 2023. DOI: <http://doi.org/10.17190/AMF/1985438>.
- 773 [171] N. (E. O. Network), “AmeriFlux FLUXNET-1F US-xUN NEON University of Notre Dame
774 Environmental Research Center (UNDE), Ver. 3-5,” *AmeriFlux AMP*, 2023. DOI: <http://doi.org/10.17190/AMF/1985458>.
- 775 [172] M. Goulden, “AmeriFlux FLUXNET-1F CA-NS6 UCI-1989 burn site, Ver. 3-5,” *AmeriFlux*
776 *AMP*, 2022. DOI: <http://doi.org/10.17190/AMF/1902829>.
- 777 [173] *no_info_available*, “*no_info_available*,” *no_info_available*, *no_info_available*. DOI: *no_info_*
778 *available*.
- 779 [174] R. Bracho, G. Celis, H. Rodenhizer, C. See, and E. A. Schuur, “AmeriFlux FLUXNET-1F
780 US-EML Eight Mile Lake Permafrost thaw gradient, Healy Alaska., Ver. 3-5,” *AmeriFlux*
781 *AMP*, 2023. DOI: <http://doi.org/10.17190/AMF/2007170>.
- 782 [175] M. Ueyama, H. Iwata, and Y. Harazono, “AmeriFlux FLUXNET-1F US-Fcr Cascaden Ridge
783 Fire Scar, Ver. 3-5,” *AmeriFlux AMP*, 2023. DOI: <http://doi.org/10.17190/AMF/2007172>.
- 784 [176] H. Liu, M. Huang, and X. Chen, “AmeriFlux FLUXNET-1F US-Hn3 Hanford 100H sage-
785 brush, Ver. 3-5,” *AmeriFlux AMP*, 2022. DOI: <http://doi.org/10.17190/AMF/1881580>.
- 786 [177] E. Euskirchen, G. Shaver, and S. Bret-Harte, “AmeriFlux FLUXNET-1F US-ICb Imnavait
787 Creek Watershed Heath Tundra, Ver. 3-5,” *AmeriFlux AMP*, 2023. DOI: <http://doi.org/10.17190/AMF/2007175>.
- 788 [178] E. Euskirchen, G. Shaver, and S. Bret-Harte, “AmeriFlux FLUXNET-1F US-ICt Imnavait
789 Creek Watershed Tussock Tundra, Ver. 3-5,” *AmeriFlux AMP*, 2022. DOI: <http://doi.org/10.17190/AMF/1881583>.
- 790 [179] C. Tweedie, “AmeriFlux FLUXNET-1F US-Jo1 Jornada Experimental Range Bajada Site,
791 Ver. 3-5,” *AmeriFlux AMP*, 2022. DOI: <http://doi.org/10.17190/AMF/1902833>.
- 792 [180] E. R. Vivoni and E. R. Perez-Ruiz, “AmeriFlux FLUXNET-1F US-Jo2 Jornada Experimental
793 Range Mixed Shrubland, Ver. 3-5,” *AmeriFlux AMP*, 2022. DOI: <http://doi.org/10.17190/AMF/1881584>.
- 794 [181] G. Flerchinger, “AmeriFlux FLUXNET-1F US-Rws Reynolds Creek Wyoming big sagebrush,
795 Ver. 3-5,” *AmeriFlux AMP*, 2022. DOI: <http://doi.org/10.17190/AMF/1881592>.
- 796 [182] S. Kurc, “AmeriFlux FLUXNET-1F US-SRC Santa Rita Creosote, Ver. 3-5,” *AmeriFlux*
797 *AMP*, 2022. DOI: <http://doi.org/10.17190/AMF/1871145>.
- 798 [183] M. Litvak, “AmeriFlux FLUXNET-1F US-Ses Sevilleta shrubland, Ver. 3-5,” *AmeriFlux*
799 *AMP*, 2023. DOI: <http://doi.org/10.17190/AMF/1984573>.
- 800 [184] R. Scott, “AmeriFlux FLUXNET-1F US-Whs Walnut Gulch Lucky Hills Shrub, Ver. 3-5,”
801 *AmeriFlux AMP*, 2023. DOI: <http://doi.org/10.17190/AMF/1984574>.
- 802 [185] J. Chen, “AmeriFlux FLUXNET-1F US-Wi6 Pine barrens 1 (PB1), Ver. 3-5,” *AmeriFlux*
803 *AMP*, 2023. DOI: <http://doi.org/10.17190/AMF/2229398>.
- 804 [186] J. Chen, “AmeriFlux FLUXNET-1F US-Wi7 Red pine clearcut (RPCC), Ver. 3-5,” *AmeriFlux*
805 *AMP*, 2023. DOI: <http://doi.org/10.17190/AMF/2229399>.
- 806 [187] N. (E. O. Network), “AmeriFlux FLUXNET-1F US-xHE NEON Healy (HEAL), Ver. 3-5,”
807 *AmeriFlux AMP*, 2023. DOI: <http://doi.org/10.17190/AMF/1985442>.
- 808 [188] N. (E. O. Network), “AmeriFlux FLUXNET-1F US-xJR NEON Jornada LTER (JORN), Ver.
809 3-5,” *AmeriFlux AMP*, 2023. DOI: <http://doi.org/10.17190/AMF/2229408>.
- 810 [189] N. (E. O. Network), “AmeriFlux FLUXNET-1F US-xMB NEON Moab (MOAB), Ver. 3-5,”
811 *AmeriFlux AMP*, 2023. DOI: <http://doi.org/10.17190/AMF/1985446>.
- 812 [190] N. (E. O. Network), “AmeriFlux FLUXNET-1F US-xNQ NEON Onaqui-Ault (ONAQ), Ver.
813 3-5,” *AmeriFlux AMP*, 2023. DOI: <http://doi.org/10.17190/AMF/1985449>.
- 814
815
816
817
818

- 819 [191] N. (E. O. Network), “AmeriFlux FLUXNET-1F US-xSR NEON Santa Rita Experimental
820 Range (SRER), Ver. 3-5,” *AmeriFlux AMP*, 2023. DOI: [http://doi.org/10.17190/AMF/](http://doi.org/10.17190/AMF/1985453)
821 1985453.
- 822 [192] R. Scott, “AmeriFlux FLUXNET-1F US-LS2 San Pedro River Lewis Springs Savanna, Ver.
823 3-5,” *AmeriFlux AMP*, 2023. DOI: [http://doi.org/10.17190/AMF/](http://doi.org/10.17190/AMF/2204870)2204870.
- 824 [193] M. Litvak, “AmeriFlux FLUXNET-1F US-Wjs Willard Juniper Savannah, Ver. 3-5,” *Ameri-*
825 *Flux AMP*, 2022. DOI: [http://doi.org/10.17190/AMF/](http://doi.org/10.17190/AMF/1871146)1871146.
- 826 [194] N. (E. O. Network), “AmeriFlux FLUXNET-1F US-xSJ NEON San Joaquin Experimental
827 Range (SJER), Ver. 3-5,” *AmeriFlux AMP*, 2023. DOI: [http://doi.org/10.17190/AMF/](http://doi.org/10.17190/AMF/2229410)
828 2229410.
- 829 [195] M. Torn and S. Dengel, “AmeriFlux FLUXNET-1F US-NGB NGEE Arctic Barrow, Ver. 3-5,”
830 *AmeriFlux AMP*, 2021. DOI: [http://doi.org/10.17190/AMF/](http://doi.org/10.17190/AMF/1832162)1832162.
- 831 [196] A. Desai, “AmeriFlux FLUXNET-1F US-Pnp Lake Mendota, Picnic Point Site, Ver. 3-5,”
832 *AmeriFlux AMP*, 2023. DOI: [http://doi.org/10.17190/AMF/](http://doi.org/10.17190/AMF/2229386)2229386.
- 833 [197] G. Bohrer, “AmeriFlux FLUXNET-1F US-UM3 Douglas Lake, Ver. 3-5,” *AmeriFlux AMP*,
834 2022. DOI: [http://doi.org/10.17190/AMF/](http://doi.org/10.17190/AMF/1881596)1881596.
- 835 [198] L. Kutzbach, “AmeriFlux FLUXNET-1F AR-TF1 Rio Moat bog, Ver. 3-5,” *AmeriFlux AMP*,
836 2021. DOI: [http://doi.org/10.17190/AMF/](http://doi.org/10.17190/AMF/1818370)1818370.
- 837 [199] A. Todd and E. Humphreys, “AmeriFlux FLUXNET-1F CA-ARB Attawapiskat River Bog,
838 Ver. 3-5,” *AmeriFlux AMP*, 2022. DOI: [http://doi.org/10.17190/AMF/](http://doi.org/10.17190/AMF/1902821)1902821.
- 839 [200] A. Todd and E. Humphreys, “AmeriFlux FLUXNET-1F CA-ARF Attawapiskat River Fen,
840 Ver. 3-5,” *AmeriFlux AMP*, 2022. DOI: [http://doi.org/10.17190/AMF/](http://doi.org/10.17190/AMF/1902822)1902822.
- 841 [201] T. Papakyriakou, “AmeriFlux FLUXNET-1F CA-CF1 Churchill Fen Site 1, Ver. 3-5,” *Ameri-*
842 *Flux AMP*, 2023. DOI: [http://doi.org/10.17190/AMF/](http://doi.org/10.17190/AMF/2229375)2229375.
- 843 [202] S. Knox, “AmeriFlux FLUXNET-1F CA-DB2 Delta Burns Bog 2, Ver. 3-5,” *AmeriFlux AMP*,
844 2022. DOI: [http://doi.org/10.17190/AMF/](http://doi.org/10.17190/AMF/1881564)1881564.
- 845 [203] A. Christen and S. Knox, “AmeriFlux FLUXNET-1F CA-DBB Delta Burns Bog, Ver. 3-5,”
846 *AmeriFlux AMP*, 2022. DOI: [http://doi.org/10.17190/AMF/](http://doi.org/10.17190/AMF/1881565)1881565.
- 847 [204] T. Roman, T. Griffis, R. Kolka, *et al.*, “AmeriFlux FLUXNET-1F PE-QFR Quistococha
848 Forest Reserve, Ver. 3-5,” *AmeriFlux AMP*, 2021. DOI: [http://doi.org/10.17190/AMF/](http://doi.org/10.17190/AMF/1832157)
849 1832157.
- 850 [205] B. Olson, “AmeriFlux FLUXNET-1F US-ALQ Allequash Creek Site, Ver. 3-5,” *AmeriFlux*
851 *AMP*, 2023. DOI: [http://doi.org/10.17190/AMF/](http://doi.org/10.17190/AMF/2006964)2006964.
- 852 [206] E. Euskirchen, “AmeriFlux FLUXNET-1F US-BZB Bonanza Creek Thermokarst Bog, Ver.
853 3-5,” *AmeriFlux AMP*, 2022. DOI: [http://doi.org/10.17190/AMF/](http://doi.org/10.17190/AMF/1881569)1881569.
- 854 [207] E. Euskirchen, “AmeriFlux FLUXNET-1F US-BZF Bonanza Creek Rich Fen, Ver. 3-5,”
855 *AmeriFlux AMP*, 2022. DOI: [http://doi.org/10.17190/AMF/](http://doi.org/10.17190/AMF/1881570)1881570.
- 856 [208] E. Euskirchen, “AmeriFlux FLUXNET-1F US-BZo Bonanza Creek Old Thermokarst Bog,
857 Ver. 3-5,” *AmeriFlux AMP*, 2022. DOI: [http://doi.org/10.17190/AMF/](http://doi.org/10.17190/AMF/1881571)1881571.
- 858 [209] P. Oikawa, “AmeriFlux FLUXNET-1F US-EDN Eden Landing Ecological Reserve, Ver. 3-5,”
859 *AmeriFlux AMP*, 2021. DOI: [http://doi.org/10.17190/AMF/](http://doi.org/10.17190/AMF/1832159)1832159.
- 860 [210] J. D. Forsythe, M. A. Kline, and T. L. O’Halloran, “AmeriFlux FLUXNET-1F US-HB1
861 North Inlet Crab Haul Creek, Ver. 3-5,” *AmeriFlux AMP*, 2021. DOI: [http://doi.org/10.17190/AMF/](http://doi.org/10.17190/AMF/1832160)
862 1832160.
- 863 [211] E. Euskirchen, G. Shaver, and S. Bret-Harte, “AmeriFlux FLUXNET-1F US-ICs Imnavait
864 Creek Watershed Wet Sedge Tundra, Ver. 3-5,” *AmeriFlux AMP*, 2022. DOI: [http://doi.org/10.17190/AMF/](http://doi.org/10.17190/AMF/1871138)1871138.
- 865
866 [212] R. Bracho and C. R. Hinkle, “AmeriFlux FLUXNET-1F US-KS3 Kennedy Space Center
867 (salt marsh), Ver. 3-5,” *AmeriFlux AMP*, 2022. DOI: [http://doi.org/10.17190/AMF/](http://doi.org/10.17190/AMF/1881586)
868 1881586.

- 869 [213] J. H. Matthes, C. Sturtevant, P. Oikawa, *et al.*, “AmeriFlux FLUXNET-1F US-Myb Mayberry
870 Wetland, Ver. 3-5,” *AmeriFlux AMP*, 2022. DOI: [http://doi.org/10.17190/AMF/](http://doi.org/10.17190/AMF/1871139)
871 1871139.
- 872 [214] A. Noormets, J. King, B. Mitra, *et al.*, “AmeriFlux FLUXNET-1F US-NC4
873 NC *Alligator River*, Ver.3 – 5,” *AmeriFlux AMP*, 2022. DOI: [http://doi.org/10.](http://doi.org/10.17190/AMF/1902837)
874 17190/AMF/1902837.
- 875 [215] G. Bohrer, “AmeriFlux FLUXNET-1F US-ORv Olentangy River Wetland Research Park,
876 Ver. 3-5,” *AmeriFlux AMP*, 2021. DOI: <http://doi.org/10.17190/AMF/1832164>.
- 877 [216] G. Bohrer and J. Kerns, “AmeriFlux FLUXNET-1F US-OWC Old Woman Creek, Ver. 3-5,”
878 *AmeriFlux AMP*, 2022. DOI: <http://doi.org/10.17190/AMF/1871142>.
- 879 [217] B. Bergamaschi and L. Windham-Myers, “AmeriFlux FLUXNET-1F US-Srr Suisun marsh -
880 Rush Ranch, Ver. 3-5,” *AmeriFlux AMP*, 2023. DOI: [http://doi.org/10.17190/AMF/](http://doi.org/10.17190/AMF/2229389)
881 2229389.
- 882 [218] R. Vargas, “AmeriFlux FLUXNET-1F US-StJ St Jones Reserve, Ver. 3-5,” *AmeriFlux AMP*,
883 2023. DOI: <http://doi.org/10.17190/AMF/2229390>.
- 884 [219] A. Valach, R. Shortt, D. Szutu, *et al.*, “AmeriFlux FLUXNET-1F US-Tw1 Twitchell Wetland
885 West Pond, Ver. 3-5,” *AmeriFlux AMP*, 2021. DOI: [http://doi.org/10.17190/AMF/](http://doi.org/10.17190/AMF/1832165)
886 1832165.
- 887 [220] E. Eichelmann, R. Shortt, S. Knox, *et al.*, “AmeriFlux FLUXNET-1F US-Tw4 Twitchell East
888 End Wetland, Ver. 3-5,” *AmeriFlux AMP*, 2023. DOI: [http://doi.org/10.17190/AMF/](http://doi.org/10.17190/AMF/2204881)
889 2204881.
- 890 [221] A. Valach, K. Kasak, D. Szutu, J. Verfaillie, and D. Baldocchi, “AmeriFlux FLUXNET-1F
891 US-Tw5 East Pond Wetland, Ver. 3-5,” *AmeriFlux AMP*, 2022. DOI: [http://doi.org/10.](http://doi.org/10.17190/AMF/1881595)
892 17190/AMF/1881595.
- 893 [222] J. Chen and H. Chu, “AmeriFlux FLUXNET-1F US-WPT Winous Point North Marsh, Ver.
894 3-5,” *AmeriFlux AMP*, 2023. DOI: <http://doi.org/10.17190/AMF/2229402>.
- 895 [223] N. (E. O. Network), “AmeriFlux FLUXNET-1F US-xBA NEON Barrow Environmental
896 Observatory (BARR), Ver. 3-5,” *AmeriFlux AMP*, 2023. DOI: [http://doi.org/10.17190/](http://doi.org/10.17190/AMF/2229404)
897 AMF/2229404.
- 898 [224] G. Vourlitis, H. Dalmagro, J. de S. Nogueira, M. Johnson, and P. Arruda, “AmeriFlux
899 FLUXNET-1F BR-Npw Northern Pantanal Wetland, Ver. 3-5,” *AmeriFlux AMP*, 2022. DOI:
900 <http://doi.org/10.17190/AMF/1881563>.

Checklist

1. For all authors...
 - (a) Do the main claims made in the abstract and introduction accurately reflect the paper's contributions and scope? **[Yes]**
 - (b) Did you describe the limitations of your work? **[Yes]** See 6
 - (c) Did you discuss any potential negative societal impacts of your work? **[Yes]** Our limitations cover this
 - (d) Have you read the ethics review guidelines and ensured that your paper conforms to them? **[TODO]** Still need to properly document all code
2. If you are including theoretical results...
 - (a) Did you state the full set of assumptions of all theoretical results? **[N/A]**
 - (b) Did you include complete proofs of all theoretical results? **[N/A]**
3. If you ran experiments (e.g. for benchmarks)...
 - (a) Did you include the code, data, and instructions needed to reproduce the main experimental results (either in the supplemental material or as a URL)? **[TODO]**
 - (b) Did you specify all the training details (e.g., data splits, hyperparameters, how they were chosen)? **[TODO]** Briefly discussed in section 5, but need to finish details in appendices / supplementary
 - (c) Did you report error bars (e.g., with respect to the random seed after running experiments multiple times)? **[No]** The error bars with different seeds were very small and were not visible in our figures
 - (d) Did you include the total amount of compute and the type of resources used (e.g., type of GPUs, internal cluster, or cloud provider)? **[Yes]** See section 5
4. If you are using existing assets (e.g., code, data, models) or curating/releasing new assets...
 - (a) If your work uses existing assets, did you cite the creators? **[Yes]** See section 3.1 for data attributions. Appendix contains full EC site list.
 - (b) Did you mention the license of the assets? **[Yes]** Section 3.3 has info on licensing of EC data and MODIS data
 - (c) Did you include any new assets either in the supplemental material or as a URL? **[TODO]**
 - (d) Did you discuss whether and how consent was obtained from people whose data you're using/curating? **[N/A]** Covered under licensing
 - (e) Did you discuss whether the data you are using/curating contains personally identifiable information or offensive content? **[N/A]** Our dataset contains no PII.
5. If you used crowdsourcing or conducted research with human subjects...
 - (a) Did you include the full text of instructions given to participants and screenshots, if applicable? **[N/A]**
 - (b) Did you describe any potential participant risks, with links to Institutional Review Board (IRB) approvals, if applicable? **[N/A]**
 - (c) Did you include the estimated hourly wage paid to participants and the total amount spent on participant compensation? **[N/A]**

Appendices

A Eddy Covariance Site Details

Here we provide an exhaustive list of EC sites used in CarbonSense along with their most recent publication. As per Ameriflux’s data policy, each site has an individual citation with DOI; other networks simply required citation of the unified release. It would be impractical to have each site’s full description in these tables, but the first two letters of each code represent the country where the site is located (ex. "DE" for Germany).

We also enumerate all meteorological predictors and targets in table 6.

Table 3: EC Sites

Croplands (CRO)					
BE-Lon [22]	CA-ER1 [32]	CA-MA1 [33]	CA-MA2 [34]	CH-Oe2 [23]	CZ-KrP [23]
DE-Geb [22]	DE-Kli [22]	DE-RuS [22]	DE-Seh [16]	DK-Fou [16]	DK-Vng [22]
FI-Jok [16]	FI-Qvd [23]	FR-Aur [22]	FR-EM2 [22]	FR-Gri [22]	FR-Lam [22]
IT-BCi [23]	IT-CA2 [16]	US-A74 [35]	US-ARM [36]	US-Bi1 [37]	US-Bi2 [38]
US-CF1 [39]	US-CF2 [40]	US-CF3 [41]	US-CF4 [42]	US-CRT [43]	US-CS1 [44]
US-CS3 [45]	US-CS4 [46]	US-DFC [47]	US-DS3 [48]	US-Lin [49]	US-Mo1 [50]
US-Mo3 [51]	US-Ne1 [52]	US-RGA [53]	US-RGB [54]	US-RGo [55]	US-Ro1 [56]
US-Ro2 [57]	US-Ro5 [58]	US-Ro6 [59]	US-Tw2 [60]	US-Tw3 [61]	US-Twt [16]
US-xSL [62]					
Closed Shrublands (CSH)					
BE-Maa [22]	IT-Noe [16]	US-KS2 [63]	US-Rls [64]	US-Rms [65]	US-Rwe [66]
US-Rwf [67]					
Cropland/Natural Vegetation Mosaics (CVM)					
US-HWB [68]	US-xDS [69]				
Deciduous Broadleaf Forests (DBF)					
AU-Lox [16]	BE-Lcr [22]	CA-Cbo [70]	CA-Oas [16]	CA-TPD [71]	CZ-Lnz [22]
CZ-Stn [23]	DE-Hai [22]	DE-Hzd [23]	DE-Lnf [16]	DK-Sor [22]	FR-Fon [22]
FR-Hes [22]	IT-BFt [22]	IT-CA1 [16]	IT-CA3 [16]	IT-Col [16]	IT-Isp [16]
IT-PT1 [16]	IT-Ro1 [16]	IT-Ro2 [16]	JP-MBF [16]	MX-Tes [72]	PA-SPn [16]
US-Bar [73]	US-Ha1 [74]	US-MMS [75]	US-MOz [76]	US-Oho [77]	US-Rpf [78]
US-UMB [79]	US-UMd [80]	US-WCr [16]	US-Wi1 [81]	US-Wi3 [82]	US-Wi8 [83]
US-xBL [84]	US-xBR [85]	US-xGR [86]	US-xHA [87]	US-xML [88]	US-xSC [89]
US-xSE [90]	US-xST [91]	US-xTR [92]	US-xUK [93]	ZM-Mon [16]	
Deciduous Needleleaf Forests (DNF)					
BR-CST [94]					
Evergreen Broadleaf Forests (EBF)					
AU-Cum [16]	AU-Rob [16]	AU-Wac [16]	AU-Whr [16]	AU-Wom [16]	BR-Sa3 [16]
CN-Din [16]	FR-Pue [22]	GF-Guy [22]	GH-Ank [16]	IT-Cp2 [22]	IT-Cpz [16]
MY-PSO [16]					

Table 4: EC Sites (cont'd)

Evergreen Needleleaf Forests (ENF)					
AR-Vir [16]	CA-Ca1 [95]	CA-Ca2 [96]	CA-LP1 [97]	CA-Man [16]	CA-NS1 [98]
CA-NS2 [99]	CA-NS3 [100]	CA-NS4 [101]	CA-NS5 [102]	CA-Obs [16]	CA-Qfo [103]
CA-SF1 [104]	CA-SF2 [105]	CA-TP1 [106]	CA-TP2 [16]	CA-TP3 [107]	CA-TP4 [16]
CH-Dav [22]	CN-Qia [16]	CZ-BK1 [22]	CZ-RAJ [23]	DE-Lkb [16]	DE-Msr [22]
DE-Obe [23]	DE-RuW [22]	DE-Tha [22]	DK-Gds [22]	FI-Hyy [22]	FI-Ken [22]
FI-Let [22]	FI-Sod [16]	FI-Var [22]	FR-Bil [22]	FR-FBn [23]	FR-LBr [16]
IL-Yat [23]	IT-La2 [16]	IT-Lav [23]	IT-Ren [22]	IT-SR2 [22]	IT-SRo [16]
NL-Loo [16]	RU-Fy2 [23]	RU-Fyo [23]	SE-Htm [22]	SE-Nor [22]	SE-Ros [23]
SE-Svb [22]	US-BZS [108]	US-Blo [16]	US-CS2 [109]	US-Fmf [110]	US-Fuf [111]
US-GBT [16]	US-GLE [112]	US-HB2 [113]	US-HB3 [114]	US-Ho2 [115]	US-KS1 [116]
US-Me1 [117]	US-Me2 [118]	US-Me3 [119]	US-Me4 [16]	US-Me5 [16]	US-Me6 [120]
US-NC1 [121]	US-NC3 [122]	US-NR1 [123]	US-Prr [16]	US-Vcm [124]	US-Vcp [125]
US-Wi0 [126]	US-Wi2 [16]	US-Wi4 [127]	US-Wi5 [128]	US-Wi9 [129]	US-xAB [130]
US-xBN [131]	US-xDJ [132]	US-xJE [133]	US-xRM [134]	US-xSB [135]	US-xTA [136]
US-xYE [137]					
Grasslands (GRA)					
AT-Neu [16]	AU-DaP [16]	AU-Emr [16]	AU-Rig [16]	AU-Stp [16]	AU-TTE [16]
AU-Ync [16]	BE-Dor [23]	CA-MA3 [138]	CH-Aws [23]	CH-Cha [23]	CH-Fru [23]
CH-Oe1 [16]	CN-Cng [16]	CN-Dan [16]	CN-Du2 [16]	CN-Du3 [16]	CN-HaM [16]
CN-Sw2 [16]	CZ-BK2 [16]	DE-Gri [22]	DE-RuR [22]	DK-Eng [16]	FR-Mej [22]
FR-Tou [22]	GL-ZaH [22]	IT-MBo [23]	IT-Niv [22]	IT-Tor [22]	NL-Hor [16]
PA-SPs [16]	RU-Ha1 [16]	SE-Deg [22]	US-A32 [139]	US-AR1 [140]	US-AR2 [141]
US-ARb [142]	US-ARc [143]	US-BRG [144]	US-Cop [145]	US-Goo [16]	US-Hn2 [146]
US-IB2 [16]	US-KFS [147]	US-KLS [148]	US-Kon [149]	US-Mo2 [150]	US-NGC [151]
US-ONA [152]	US-Ro4 [153]	US-SRG [154]	US-Seg [155]	US-Sne [156]	US-Snf [157]
US-Var [158]	US-Wkg [159]	US-xAE [160]	US-xCL [161]	US-xCP [162]	US-xDC [163]
US-xKA [164]	US-xKZ [165]	US-xNG [166]	US-xWD [167]		
Mixed Forests (MF)					
AR-SLu [16]	BE-Bra [22]	BE-Vie [22]	CA-Gro [168]	CD-Ygb [22]	CH-Lae [23]
CN-Cha [16]	DE-Har [22]	DE-HoH [22]	JP-SMF [16]	US-Syv [169]	US-xDL [170]
US-xUN [171]					
Open Shrublands (OSH)					
CA-NS6 [172]	CA-NS7 [173]	CA-SF3 [16]	ES-Agu [23]	ES-Amo [16]	ES-LJu [23]
ES-LgS [16]	ES-Ln2 [16]	GL-Dsk [22]	IT-Lsn [22]	RU-Cok [16]	US-EML [174]
US-Fcr [175]	US-Hn3 [176]	US-ICH [177]	US-ICt [178]	US-Jo1 [179]	US-Jo2 [180]
US-Rws [181]	US-SRC [182]	US-Ses [183]	US-Sta [16]	US-Whs [184]	US-Wi6 [185]
US-Wi7 [186]	US-xHE [187]	US-xJR [188]	US-xMB [189]	US-xNQ [190]	US-xSR [191]
Savannas (SAV)					
AU-ASM [16]	AU-Cpr [16]	AU-DaS [16]	AU-Dry [16]	AU-GWW [16]	CG-Tch [16]
ES-Abr [23]	ES-LM1 [23]	ES-LM2 [23]	SD-Dem [16]	SN-Dhr [16]	US-LS2 [192]
US-Wjs [193]	US-xSJ [194]				
Snow and Ice (SNO)					
US-NGB [195]					

Table 5: EC Sites (cont'd)

Water Bodies (WAT)					
US-Pnp [196]	US-UM3 [197]				
Permanent Wetlands (WET)					
AR-TF1 [198]	AU-Fog [16]	CA-ARB [199]	CA-ARF [200]	CA-CF1 [201]	CA-DB2 [202]
CA-DBB [203]	CN-Ha2 [16]	CZ-wet [22]	DE-Akm [23]	DE-SfN [16]	DE-Spw [16]
DE-Zrk [16]	DK-Skj [22]	FI-Lom [16]	FI-Sii [22]	FR-LGt [22]	GL-NuF [22]
GL-ZaF [16]	IE-Cra [23]	PE-QFR [204]	RU-Che [16]	SE-Sto [22]	SJ-Adv [16]
UK-AMo [22]	US-ALQ [205]	US-Atq [16]	US-BZB [206]	US-BZF [207]	US-BZo [208]
US-EDN [209]	US-HB1 [210]	US-ICs [211]	US-Ivo [16]	US-KS3 [212]	US-Los [16]
US-Myb [213]	US-NC4 [214]	US-ORv [215]	US-OWC [216]	US-Srr [217]	US-StJ [218]
US-Tw1 [219]	US-Tw4 [220]	US-Tw5 [221]	US-WPT [222]	US-xBA [223]	
Woody Savannas (WSA)					
AU-Ade [16]	AU-Gin [16]	AU-How [16]	AU-RDF [16]	BR-Npw [224]	ES-Cnd [23]

Table 6: Meteorological Variables in CarbonSense

Code	Description	Units
Predictors		
TA_F	Air temperature	deg C
PA_F	Atmospheric pressure	kPa
P_F	Precipitation	mm
RH	Relative humidity	%
VPD_F	Vapor pressure deficit	hPa
WS_F	Wind speed	m s ⁻¹
WD	Wind direction	decimal degrees
USTAR	Frictional wind velocity	m s ⁻¹
NETRAD	Net radiation	W m ⁻²
SW_IN_F	Incoming shortwave radiation	W m ⁻²
SW_OUT	Outgoing shortwave radiation	W m ⁻²
SW_DIF	Incoming diffuse shortwave radiation	W m ⁻²
LW_IN_F	Incoming longwave radiation	W m ⁻²
LW_OUT	Outgoing longwave radiation	W m ⁻²
PPFD_IN	Incoming photosynthetic photon flux density	μmol Photon m ⁻² s ⁻¹
PPFD_OUT	Outgoing photosynthetic photon flux density	μmol Photon m ⁻² s ⁻¹
PPFD_DIF	Incoming diffuse photosynthetic photon flux density	μmol Photon m ⁻² s ⁻¹
CO2_F_MDS	CO2 atmospheric concentration	μmol CO ₂ mol ⁻¹
G_F_MDS	Soil heat flux	W m ⁻²
LE_F_MDS	Latent heat flux	W m ⁻²
H_F_MDS	Sensible heat flux	W m ⁻²
Targets		
NEE_VUT_REF	Net Ecosystem Exchange (variable USTAR)	μmol CO ₂ m ⁻² s ⁻¹
GPP_DT_VUT_REF	Gross Primary Production (daytime partitioning)	μmol CO ₂ m ⁻² s ⁻¹
GPP_NT_VUT_REF	Gross Primary Production (nighttime partitioning)	μmol CO ₂ m ⁻² s ⁻¹
RECO_DT_VUT_REF	Ecosystem Respiration (daytime partitioning)	μmol CO ₂ m ⁻² s ⁻¹
RECO_NT_VUT_REF	Ecosystem Respiration (nighttime partitioning)	μmol CO ₂ m ⁻² s ⁻¹

